Supporting Information

Enhanced Depolymerization of Poly(Bisphenol A Carbonate) via Robust Mesoporous $CaCO_3/CaTiO_3$ Nanocomposites Featuring Synergistic Acid–Base Sites and Oxygen Vacancies

Shuoxian Li,[a] Tao Song,*[a] Yi Sun,[a], Hongbin Hou,[a] Guangqian Zhu,*[b,c] Liang Wang,*[b,c] Qinggang Wang, Guangqiang Xu*[b,c]

[a]Qingdao New Energy Shandong Laboratory, Qingdao Institute of Bioenergy and Bioprocess Technology, Chinese Academy of Sciences, Qingdao 266101, China

[b]Shandong Energy Institute, Qingdao 266101, China

[c]Qingdao Institute of Bioenergy and Bioprocess Technology, Chinese Academy of Sciences, Qingdao 266101, China

* Corresponding author

E-mail: songtao@qibebt.ac.cn, zhugq@qibebt.ac.cn, wangliang@qibebt.ac.cn, xu_gq@qibebt.ac.cn

1. General information

Catalyst characterization

A comprehensive suite of physicochemical characterization techniques was employed to elucidate the structural, morphological, and surface properties of the synthesized catalysts, thereby establishing correlations between structure and catalytic activity. The crystalline phase composition was analyzed by X-ray diffraction (XRD) using a SmartLab 9 kW diffractometer (Rigaku, Japan) with Cu Kα radiation (λ = 0.15 nm) over a 2θ range of 10°–90°, with a scan rate of 20° min^{-1} and a step size of 0.02°. The surface morphology was examined via scanning electron microscopy (SEM) on a Hitachi S-4800 field-emission microscope after gold sputtering, under a 15 kV accelerating voltage, to observe particle size, surface texture, and porosity. High-resolution transmission electron microscopy (HR-TEM) was performed on a Tecnai G2 F20 (FEI, USA) operated at 200 kV; samples were ultrasonically dispersed in ethanol, deposited onto carbon-coated copper grids, and dried at room temperature to assess lattice fringes and phase distribution. X-ray photoelectron spectroscopy (XPS) was conducted on an AXIS SUPRA+ (Shimadzu, Japan) with a monochromated Al Kα source (hν = 1486.6 eV) under < 10^{-7} Pa chamber pressure, with all binding energies referenced to the C 1s peak at 284.6 eV, to determine surface composition and oxidation states. Nitrogen adsorption–desorption (BET/BJH) measurements were carried out using an ASAP 2460 analyzer (Micromeritics, USA) after degassing at 200 °C for 6 h, to calculate the specific surface area and pore size distribution at −196 °C. The surface acidity and basicity were quantified through temperature-programmed desorption (TPD) using NH_3-TPD and CO_2-TPD on an AutoChem II 2920 (Micromeritics, USA). For NH_3-TPD, samples were pretreated at 500 °C in He (50 mL min^{-1}) for 1 h, adsorbed with NH_3 at 100 °C for 30 min, purged, and then heated to 700 °C at

10 °C min^{-1} under TCD detection; the CO_2-TPD procedure followed similarly with adsorption at 50 °C. Pyridine-adsorbed FTIR (Py-IR) spectra were collected using a Tensor 27 (Bruker, Germany) at 4 cm^{-1} resolution with 32 scans. Self-supported wafers (~13 mm) were pretreated under 10^{-3} Pa vacuum at 400 °C for 1 h, exposed to pyridine at room temperature for 30 min, then desorbed at 200 °C for 30 min before measurement; due to possible interference from Ca-based species, the 1100–1000 cm^{-1} region was analyzed for Lewis acid features. Finally, electron paramagnetic resonance (EPR) spectroscopy was used to investigate surface defect structures on an EMXplus X-band spectrometer (Bruker, Germany) under conditions of 3500 G central field, 1000–6000 G scan range, 9.8 GHz microwave frequency, 100 kHz modulation frequency, 1 G modulation amplitude, and 1 mW microwave power. Measurements were performed at room temperature, with additional low-temperature (77 K) scans for selected samples to enhance signal intensity.

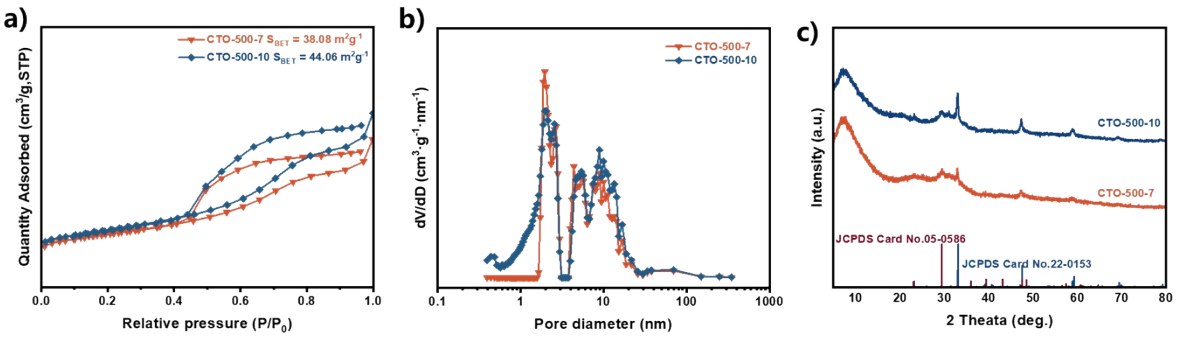

Figure S1. a) N_2 adsorption-desorption isotherms of the CTO-500-7 and CTO-500-10. b) pore-size distributions of the CTO-500-7 and CTO-500-10. c) XRD patterns of CTO-500-7 and CTO-500-10.

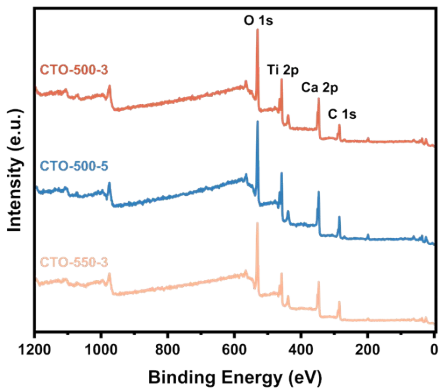

Figure S2. The XPS survey scan of CTO-500-3, CTO-500-5 and CTO-550-3.

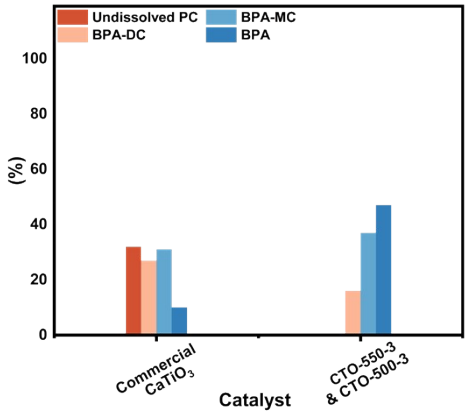

Figure S3. Catalytic performance of commercial $CaTiO_3$ and physically mixed CTO catalysts (CTO-550-3 and CTO-500-3).

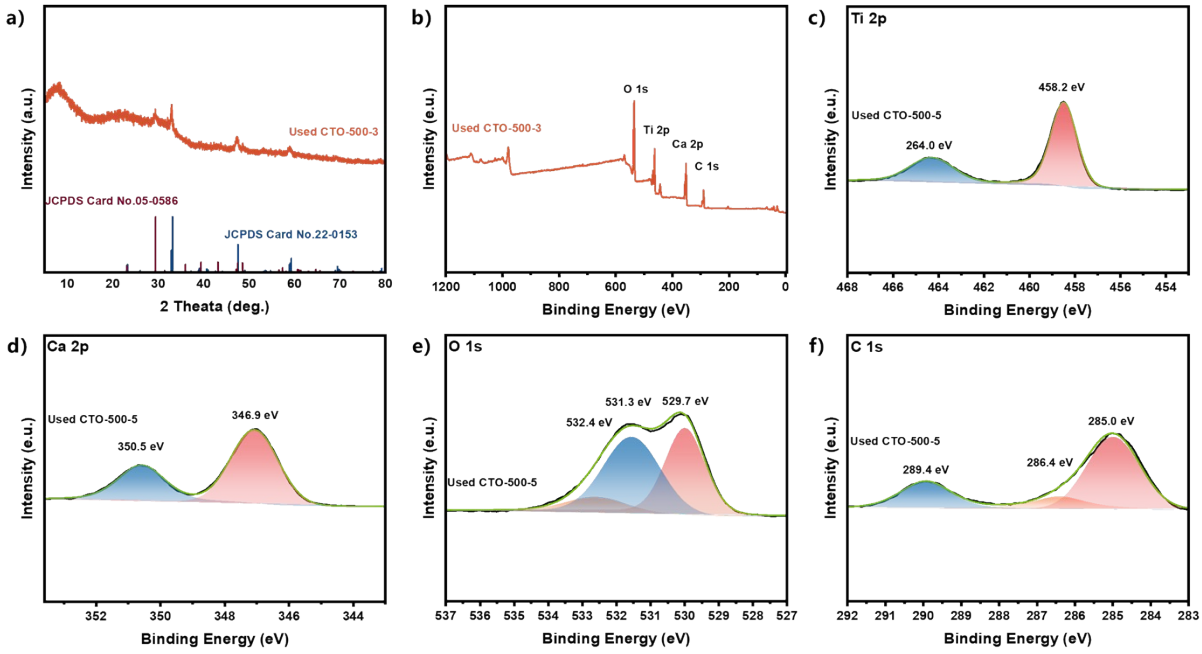

Figure S4. a) XRD, b) XPS survey scan and XPS spectra of c) Ti 2p, d) Ca 2p, e) O 1s, f) C

1s for used CTO-500-5 catalyst.

Table S1. Porosity, acid and basic properties of CTO prepared under different conditions

Sample	S_{BET}[a] ($m^2 g^{-1}$)	B_{weak}[b] (mmol g^{-1})	B_{strong}[b] (mmol g^{-1})	A_{weak}[c] (mmol g^{-1})	A_{strong}[c] (mmol g^{-1})
CTO-500-3	40.55	0.039	0.383	0.016	0.233
CTO-500-5	47.14	0.039	0.289	0.013	0.260
CTO-550-3	27.33	0.028	0.063	0.009	0.087

Lewis A_{weak}[d] (μmol g^{-1})	Lewis $A_{moderate}$[d] (μmol g^{-1})	Lewis A_{strong}[d] (μmol g^{-1})
3.29	3.31	3.29
5.40	6.00	3.00
1.80	2.50	2.91

[a]BET specific surface areas are determined with adsorption data in a relative pressure range of P/P_0 = 0.05-0.25. [b]Base amounts are determined by CO_2-TPD. [c]Acid amounts are determined by NH_3-TPD. [d]Lewis Acid amounts are determined by Py-IR.

2 · Methanolysis of BPA-PC under batch condition and product quantification methods

In a standard methanolysis of BPA-PC, BPA-PC pellets (0.50 g, 1.97 mmol repeat-unit basis), catalyst (6 wt.% relative to BPA-PC), cosolvent (1.0 mL 2-Me-THF), and anhydrous methanol (6 equiv. per repeat unit) were combined in a sealed tube and stirred at 120 °C for 4 h. After cooling, the solid catalyst was removed by vacuum filtration (100 nm nylon membrane). The recovered solid was dried and weighed to determine BPA-PC conversion. A portion of the filtrate was analyzed by ^{1}H NMR (in $CDCl_3$) to quantify BPA selectivity via integration of aromatic and isopropyl proton signals. The remaining filtrate was concentrated by rotary evaporation and dried to constant weight, yielding isolated BPA. When other alcohols were used, the procedure was adapted accordingly. If the nucleophile could not be fully removed by evaporation, BPA was purified by recrystallization: the crude product was dissolved in a

minimal amount of a good solvent, then precipitated with a large excess of a poor solvent (MeOH). Filtration and repeated recrystallization afforded pure BPA (PE).

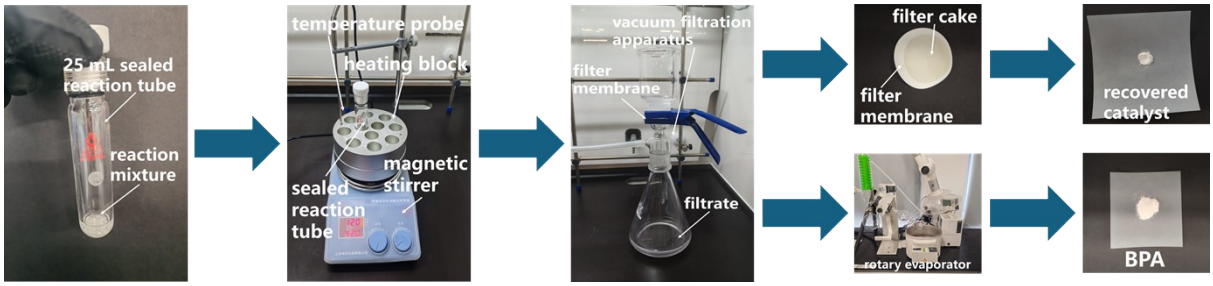

Figure S5. Schematic illustration of the experimental setup and post-treatment procedures involved in the methanolysis of BPA-PC.

After completion of the reaction, solid–liquid separation was carried out by vacuum filtration using an organic nylon membrane filter (pore size: 100 nm). The resulting solid residue was thoroughly washed and dried under appropriate conditions to constant weight, after which it was weighed to determine the conversion of BPA-PC. The conversion was calculated according to the following equation:

$$Conv.\,(\%) = \frac{m_{Initial} - m_{final}}{m_{Initial}} \times 100\%$$

Where $m_{Initial}$ is the mass of the initial reactant, and m_{final} is the mass of the unreacted reactant remaining after completion of the reaction.

The reaction filtrate was analyzed by ^{1}H NMR spectroscopy to determine the product selectivity. All ^{1}H NMR spectra were recorded on a Bruker AVANCE III 400 MHz spectrometer using deuterated chloroform ($CDCl_3$, 99.9%) as the solvent. For analysis, the reaction mixtures were appropriately diluted and transferred into 5 mm NMR tubes. The selectivity of each product was determined by integrating its characteristic proton resonances. The selectivity was calculated based on material balance according to the following equation:

$$Sel.\ (\%) = \frac{n_{product}}{n_{total}} \times 100\%$$

Where $n_{product}$is the number of moles of the target product, and n_{total} is the number of moles of the total quantity of all measured products.

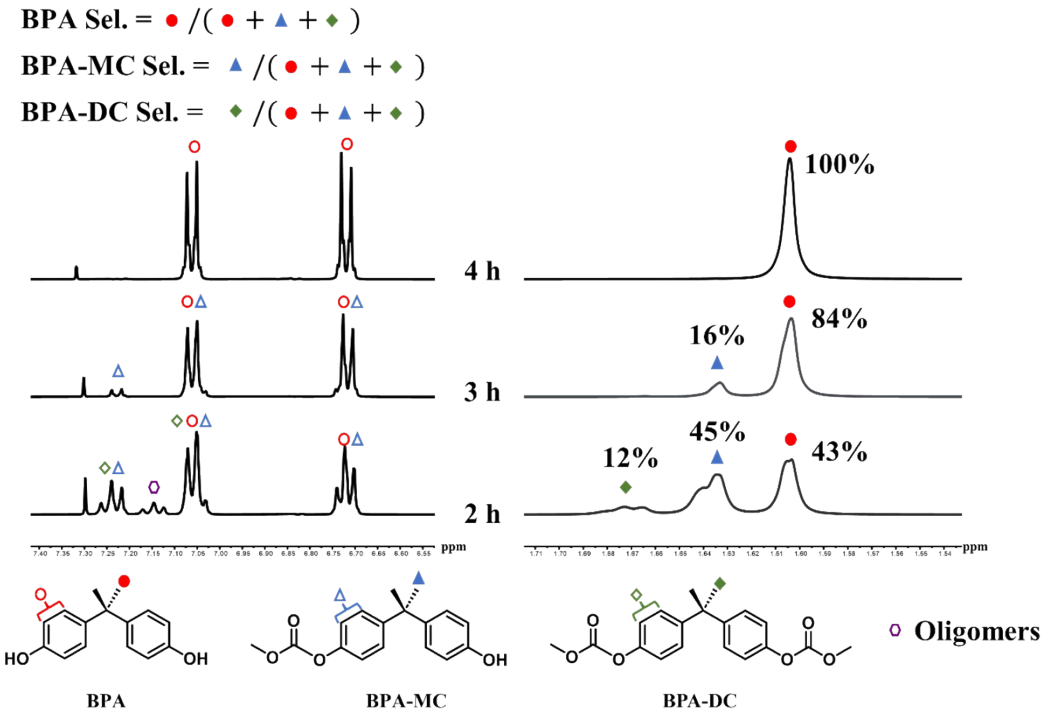

Figure S6. Calculation method of selectivity for the methanolysis of BPA-PC.

The separated filtrate was concentrated by rotary evaporation to remove residual nucleophiles and solvent, followed by further drying under reduced pressure to constant weight, with the grinding step omitted. For nucleophiles that could not be completely removed by rotary evaporation, recrystallization was employed to isolate and purify BPA. The resulting solid was collected by filtration, affording the isolated BPA product. The yield was calculated according to the following equation:

$$Yield\ (\%) = \frac{m_{product}}{m_{substrate,\,theoretical}} \times 100\%$$

Where $m_{product}$is the mass of the target product, and $m_{substrate,\,theoretical}$is the maximum theoretical mass of the product expected from the feedstock.

3. Study on the depolymerization behavior of Bisphenol A-Polycarbonate (BPA-PC)

To elaborate the depolymerization behavior of BPA-PC, the molecular weight and polydispersity were detected at various reaction times. As shown in Figure S7, during initial 1 hour of the reaction, BPA-PC was not fully dissolved, yet its Mw decreased significantly from 59,678 g/mol to 23,314 g/mol. After two hours, the BPA-PC had completely dissolved, forming oligomers with M_w = 653 g/mol. The gel permeation chromatography (GPC) profiles revealed that the elution time of BPA-PC initially fell within the range of 7.0–9.0 min. After the reaction commenced, the elution time of samples withdrawn from the system shifted markedly toward the lower molecular weight region (8.5–9.5 min, 9.5 min, and finally 10 min), demonstrating that the polymer rapidly degraded into oligomers within 2 hours. This sharp decline in molecular weight suggests that the degradation follows a random chain scission mechanism rather than a sequential unzipping depolymerization pathway (Figure R3b). Subsequently, the oligomers underwent further depolymerization into intermediate products, a process that was monitored in real time by ^{1}H NMR spectroscopy. The degradation of BPA-PC to bisphenol A (BPA) was tracked by the emergence of signals corresponding to aryl protons (6.6–6.8 ppm and 7.0–7.2 ppm) and dimethyl protons (1.6–1.7 ppm). After 2 hours of reaction, BPA-DC and BPA-MC intermediates reached yields of 12% and 43%, respectively, while the yield of BPA itself remained at only 43% (Figure S7d). As the reaction proceeded, these intermediates gradually converted into BPA monomer over time.

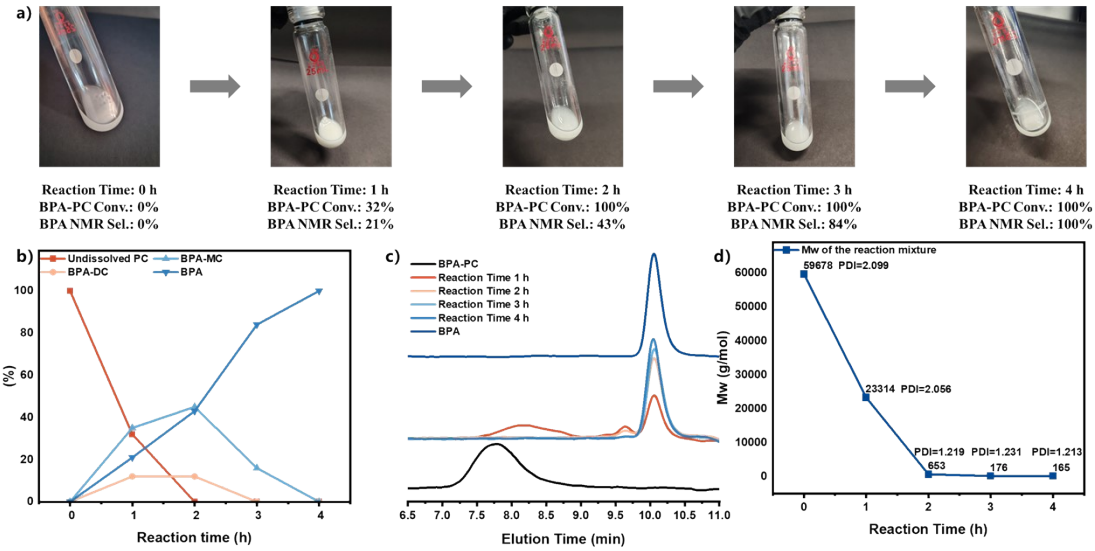

Figure S7. Time-resolved monitoring of BPA-PC methanolysis by visual observation and GPC analysis: (a) photographs of the reaction mixture at different reaction times; (b) time-dependent evolution of product composition during BPA-PC depolymerization; (c) GPC traces collected at different reaction times; and (d) time-dependent change in the *M*w of the reaction mixture.

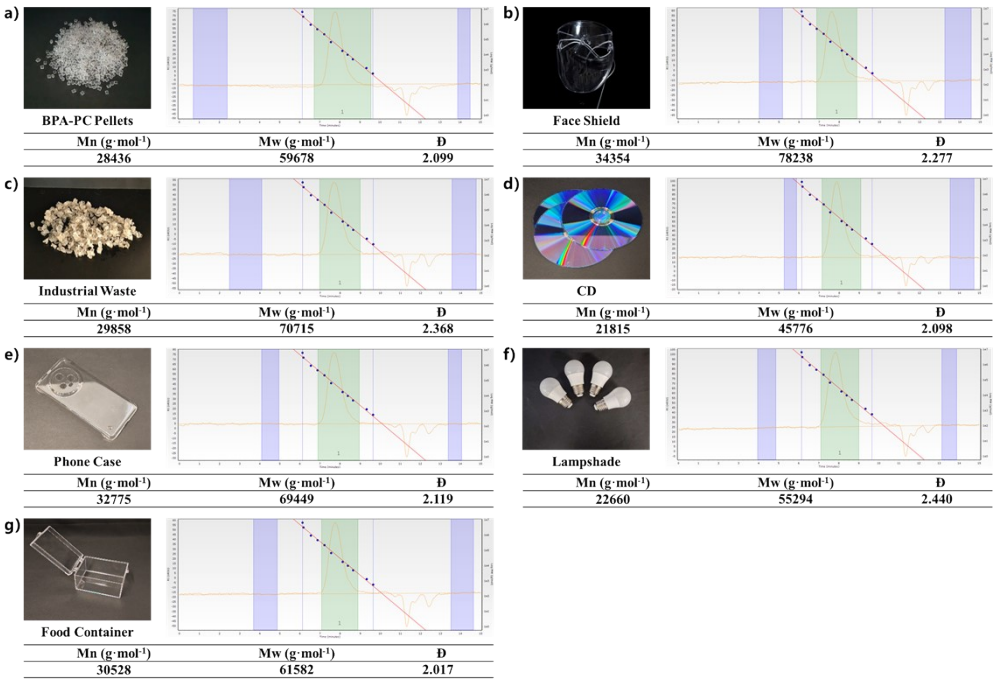

Figure S8. GPC analysis of the BPA-PC feedstock: a) BPA-PC Pellets; b) Face Shield; c) Industrial Waste; d) CD; e) Phone Case; f) Lampshade; g) Food Container.

4. Catalyst recycling under batch condition

The recyclability and stability of the $CaCO_3/CaTiO_3$ nanocatalyst were evaluated using the methanolysis of BPA-PC as a model reaction under optimized conditions. In a typical run, BPA-PC pellets (0.50 g, 1.97 mmol repeat unit), catalyst (6 wt.%), 2-Me-THF (1.0 mL), and anhydrous methanol (6 equiv.) were combined in a sealed tube and stirred at 120 °C for 4 h. After cooling, the solid catalyst was separated by vacuum filtration using a 100 nm nylon membrane. The filtrate was analyzed to determine catalytic performance.

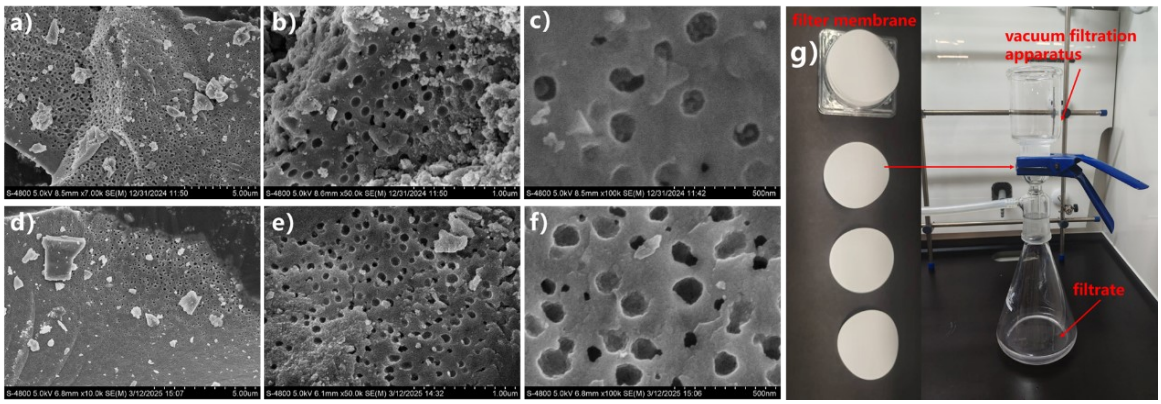

Figure S9. SEM images of the fresh catalyst (a-c) and used catalyst (d-f); (g) catalyst filtration device.

5. Expansion of catalyst applications in methanolysis and glycolysis of PET

To explore the potential application of the catalyst, we systematically evaluated its performance in the methanolysis and glycolysis of polyethylene terephthalate (PET). As shown in Figure S10, complete conversion of PET was achieved with a dimethyl terephthalate (DMT) yield of up to 98% under the optimized methanolysis conditions (0.5 g PET, 2.6 mmol; CTO-500-5, 8 wt%; methanol, 16 equiv.; 160 °C, 4 h). The catalytic system also exhibited excellent activity in the glycolysis of PET (Figure S11). Under the optimized glycolysis conditions (0.5 g PET, 2.6 mmol; CTO-500-5, 4 wt%; ethylene glycol, 8 equiv.; 180 °C, 3 h), a PET conversion of 96% and a bis(2-hydroxyethyl) terephthalate (BHET) yield of 95% were

obtained.

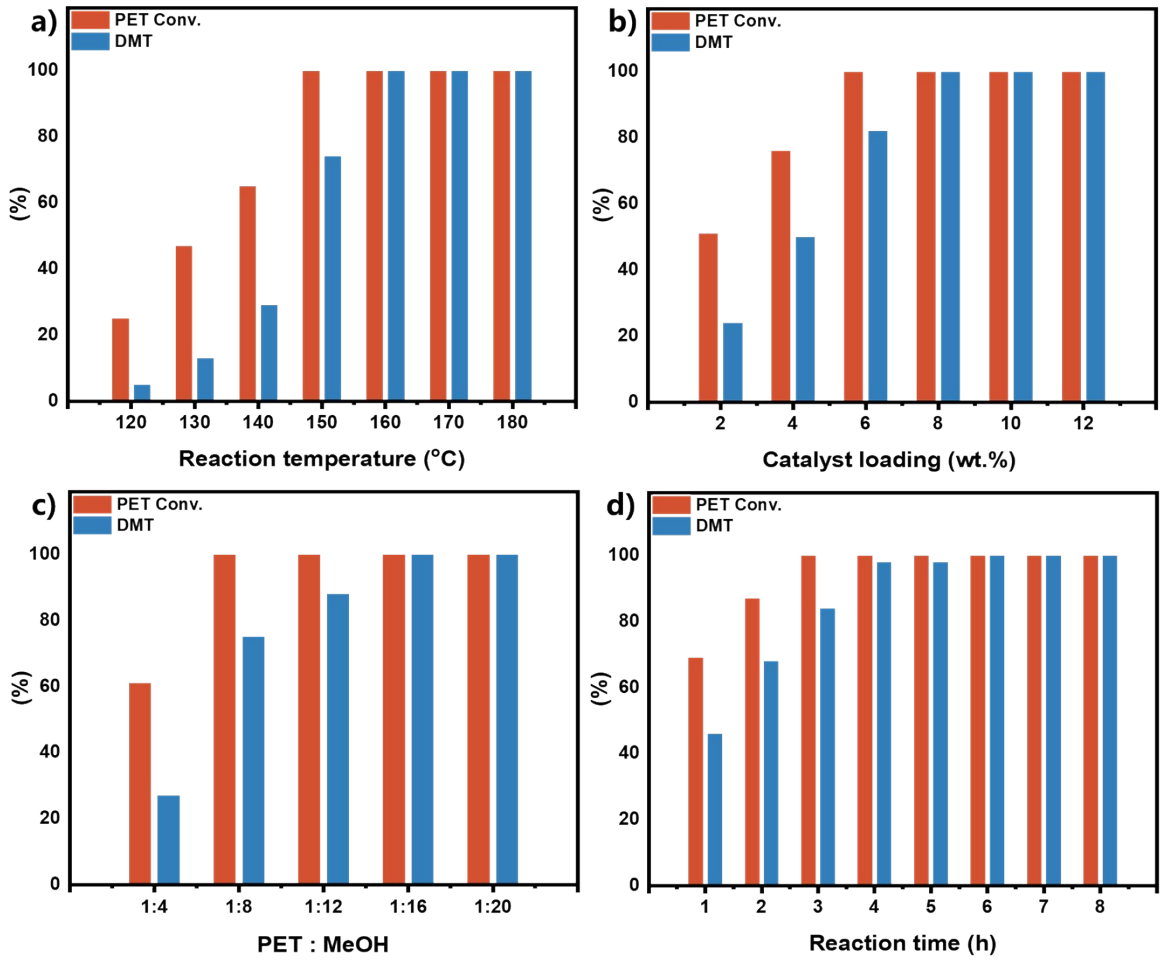

Figure S10. Reaction condition optimization for the methanolysis of PET. (a) Reaction temperature, (b) catalyst loading, (c) methanol equivalents, and (d) reaction time. [a]Reaction Condition: 0.5 g PET (2.6 mmol), CTO-500-5 (8 wt.%), 16 equiv. MeOH, 160 °C, 4 h. [b]PET conversion was determined gravimetrically by filtration and weighing of the dried solid residue. [c]DMT yield was quantified by ^{1}H NMR spectroscopy after addition of *p*-nitroacetophenone (2.6mmol) as an internal standard and dissolution in excess dichloromethane.

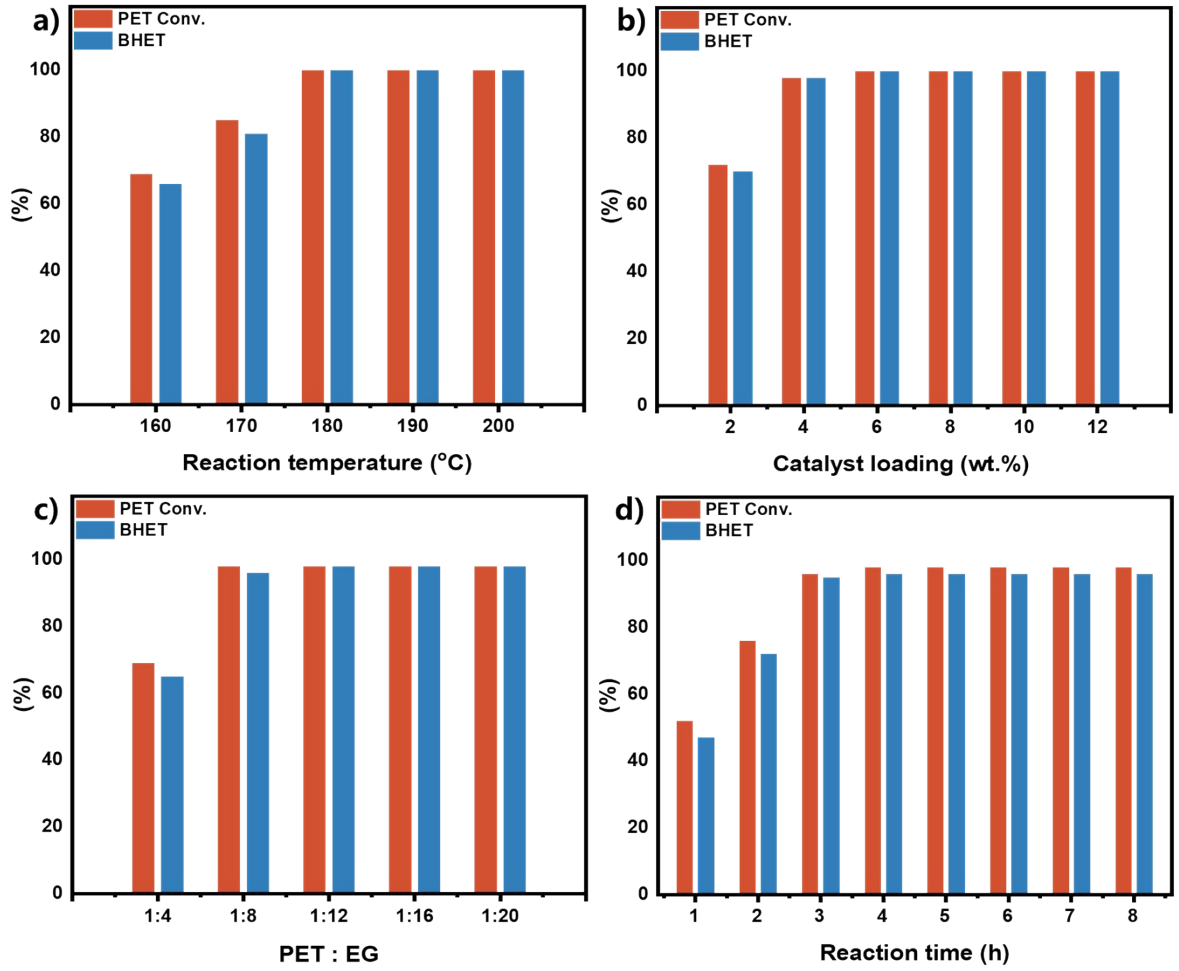

Figure S11. Reaction condition optimization for the glycolysis of PET. (a) Reaction temperature, (b) catalyst loading, (c) ethylene glycol equivalents, and (d) reaction time. [a]Reaction Condition: 0.5 g PET (2.6 mmol), CTO-500-5 (4 wt.%), 8 equiv. EG, 180 °C, 3 h. [b]PET conversion was determined gravimetrically by filtration and weighing of the dried solid residue. [c]BHET yield was determined by dissolving the reaction mixture in hot water followed by filtratio; the filtrate was extracted with dichloromethane, and the organic phase was evaporated to dryness under reduced pressure to isolate BHET.

3. The fix-bed continuous-flow reactor

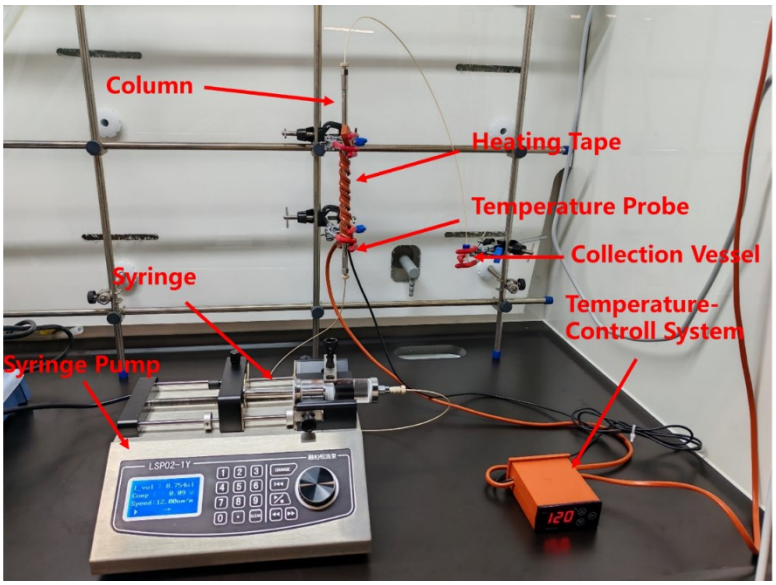

Figure S12. Fixed-bed continuous-flow equipment.

A fixed-bed continuous-flow reactor was constructed to evaluate the catalytic performance of catalysts under continuous operation. The reactor consisted of a stainless-steel chromatography column packed with 4.5 g of the catalyst CTO-500-5. Both ends of the column were sealed with frits (0.5 μm pore size) to prevent catalyst loss. The column was connected to a syringe pump and a collection vessel through 0.5 mm i.d. PEEK tubing and Luer-lock connectors.

The feed solution was prepared as follows. First, BPA-PC (1.18 mmol) was dissolved in THF as the cosolvent to obtain a 0.04 M solution (THF amount: 29.5 g), and the mixture was heated and stirred at ambient temperature until complete dissolution. Subsequently, under vigorous stirring, 30 equivalents of the nucleophile, either anhydrous methanol (1.13 g) or ethylene glycol (2.19 g), were slowly added, and the mixture was thoroughly mixed to form a homogeneous solution. The resulting solution was then allowed to stand at ambient temperature for 3 h, no solid precipitation was observed during this period.

Finally, the feed solution was continuously delivered into the catalyst bed using a syringe pump at flow rates of 5–20 μL·min^{-1} for continuous-flow reaction testing. The column was externally heated with a temperature-controlled heating tape, while the flow rate and temperature served

as the principal parameters to regulate depolymerization efficiency and product selectivity. The effluent was cooled, collected in bottles, and subjected to subsequent analysis.

4. Comparative assessment of the developed catalyst with the reported catalysts in the methanolysis of BPA-PC.

Compared with ionic liquid catalysts and immobilized homogeneous catalysts, the present catalyst exhibits comparable activity and selectivity, yet features a more straightforward and efficient preparation process. In contrast to conventional metal oxide catalysts, it can be reused for more than ten consecutive cycles without significant loss of activity or selectivity, and demonstrates long-term stable operation in fixed-bed reactions. Overall, the developed catalyst shows notable advantages in terms of synthesis simplicity, catalytic performance, and stability.

Table S2. Comparative assessment of the developed catalyst with the reported catalysts in the methanolysis of BPA-PC.

Entry	Cat.	Reaction conditions	BPA-PC Conv. (%)	BPA Yield (%)	Cat. Recycling	Ref.
1	ChCl-2Urea (DES)	BPA-PC 4 g (15.75 mmol), ChCl-2Urea (DES) 0.4 g (10 wt.% of BPA-PC), 5 eq. MeOH, 130 ℃, 2.5 h	100	100	5 times reuse BPA yield remains ~99%	*Chem. Eng. J.*, **2020**, 388, 124324
2	[EmimOH]Cl-2Urea	BPA-PC 4 g (15.75 mmol), [EmimOH]Cl-2Urea 0.4 g (10 wt.% of BPA-PC), 5 eq. MeOH, 120 ℃, 2 h	100	99	4 times reuse BPA yield from 99% to ~97%	*RSC Adv.*,**2021**,11, 1595
3	[HDBU][LAc]	BPA-PC 4 g (15.75 mmol), [HDBU][LAc] (0.8 mol% of BPA-PC), 5 eq. MeOH, 120 ℃, 1 h	100	99	6 times reuse BPA yield remains 99%	*ACS Sustain. Chem. Eng.*, **2018**, 6, 13114.
4	[Bmim][Cl]·2.0$FeCl_3$	BPA-PC 4 g (15.75 mmol), [Bmim][Cl]·2.0$FeCl_3$ (5 mol% of BPA-PC), 6 eq. MeOH, 120 ℃, 3 h	100	97.2	6 times reuse BPA yield remains 97.2%	*Ind. Eng. Chem. Res.*, **2018**, 57, 10915.
5	ZnO-NPs/NBu_4Cl	BPA-PC 0.254 g (1 mmol), Zn/BPA-PC = 5 mol%, NBu_4Cl (5 mol%), 28 eq. MeOH, 100 ℃, 7 h	>99	97	5 times reuse BPA yield from 97% to ~95%	*J. Mol. Catal. A: Chem.*, **2017**, 426, 107.
6	Fe_3O_4@SiO_2@(mim)[$ZnCl(OH)_2$]	BPA-PC 0.1 g (0.393 mmol), Fe_3O_4@SiO_2@(mim)[$ZnCl(OH)_2$] 6 mg (16.6 wt.%), 36.67 eq. EG, 180 °C (170 °C inside the reaction flask), 24 h.	>99	93	20 times reuse, BPA-PC Conv. remains at 100%, BPA yield fluctuated between 70% and 90%	*ACS Sustainable Chem. Eng.*, **2025**, 13, 7890.

7	Si-TBD	BPA-PC 2 g (7.87 mmol), Si-TBD (5 mol% of BPA-PC), 13 eq. MeOH, 65 °C, 2.5 h	100	96	10 times reuse BPA yield from 96% to 68% with catalyst regeneration	*Chem. Eng. J.*, **2024**, 485, 149832
8	DMAP @PS	BPA-PC 0.0635 g (0.25 mmol), DMAP@PS (20 mol%), DMF (0.12 M), 80 °C, 24 h.	100	>99	5 times reuse BPA-PC Conv. from 100% to ~45%	*ChemSusChem*, **2025**, 18, e202500420
9	SBA-15-Pr-MIM-OH	BPA-PC 1 g (3.93 mmol), SBA-15-Pr-MIM-OH 0.03 g (3 wt.% of BPA-PC), 11.5 eq. MeOH, 120 °C, 1 h	99.9	99.0	3 times reuse BPA yield from 100% to ~62% ; 3 times reuse BPA yield from 100% to ~93% with catalyst regeneration	*Green Chem.*, **2024**, 26, 3814.
10	10%CaO/SBA-15	BPA-PC 5 g (19.69 mmol), 10%CaO/SBA-15 1.67 g (33.33 wt.% of BPA-PC), 8 eq. MeOH, 7 eq. THF, 130 °C, 3 h	100	96.8	5 times reuse BPA yield from 98.6% to ~95%	*Catal. Letters*, **2017**, 147, 2940.
11	15%CaO/Ce-SBA-15	15%CaO/Ce-SBA-15 (30 wt.% of BPA-PC), m(MeOH):m(BPA-PC)=8:1, m(THF):m(BPA-PC)=1.5:1, 130 °C, 3 h	100	94.5	6 times reuse BPA yield from 94.5% to 92.0%	*J. Mater. Sci.*, **2019**, 54, 9442.
12	Mg_3Al-LDO	BPA-PC 4 g (15.75 mmol), Mg_3Al-LDO 0.12 g (3 wt.% of BPA-PC), 5 eq. MeOH, 110 °C, 1 h	100	98	5 times reuse BPA yield remains 98.1%	*Appl. Clay Sci.*, **2021**, 202, 105986.
13	Ca-Al_2O_3	BPA-PC 5 g (19.69 mmol), Ca-Al_2O_3 0.15 g (3 wt.% of BPA-PC), 8 eq. MeOH, 1.5 eq. THF, 130 °C, 3 h	100	96.3	6 times reuse BPA yield from 96.3% to 93.2%	*J. Taiwan Inst. Chem. Eng.*, **2018**, 86, 222.
14	ZIF-8 or MOF-5-ED	BPA-PC 2 g (7.87 mmol), ZIF-8 or MOF-5-ED 0.1 g (5 wt.% of BPA-PC), 8 eq. MeOH, 2 eq. THF, 130 °C, 3 h	ZIF-8 (95.9) MOF-5-ED (97.3)	ZIF-8 (94.1) MOF-5-ED (99.2)	ZIF-8: 3 times reuse BPA yield from 94.1% to 72.2% ; MOF-5-ED: 3 times reuse BPA yield from 99.2% to 67.2% with	*Appl. Surf. Sci.*, **2024**, 673, 160894.
15	$NaAlO_2$	BPA-PC 1 g (3.93 mmol), $NaAlO_2$ 0.2 g (20 wt.% of BPA-PC), 40 eq. MeOH, 35 eq. THF, 60 °C, 2 h	98.1	96.8	4 times reuse BPA yield from 96.8% to ~90%	*Langmuir*, **2024**, 40, 5338.
16	Y_2O_3	BPA-PC 1 g (3.93 mmol), Y_2O_3 0.02 g (2 wt.% of BPA-PC), 3.7 eq. EG, 200 °C, 2 h	100	83	no studies on cycling stability	*Eur. Polym. J.*, **2024**, 221, 113516
17	$CaCO_3$/$CaTiO_3$	BPA-PC 0.5 g (1.97 mmol), $CaCO_3$/$CaTiO_3$ 0.03 g (6 wt.% of BPA-PC), 6 eq. MeOH, 6.8 eq. 2-MeTHF, 120 °C, 4 h	100	100	10 times reuse BPA yield from 100% to 95%	This Work

5. ^{1}H NMR spectra data

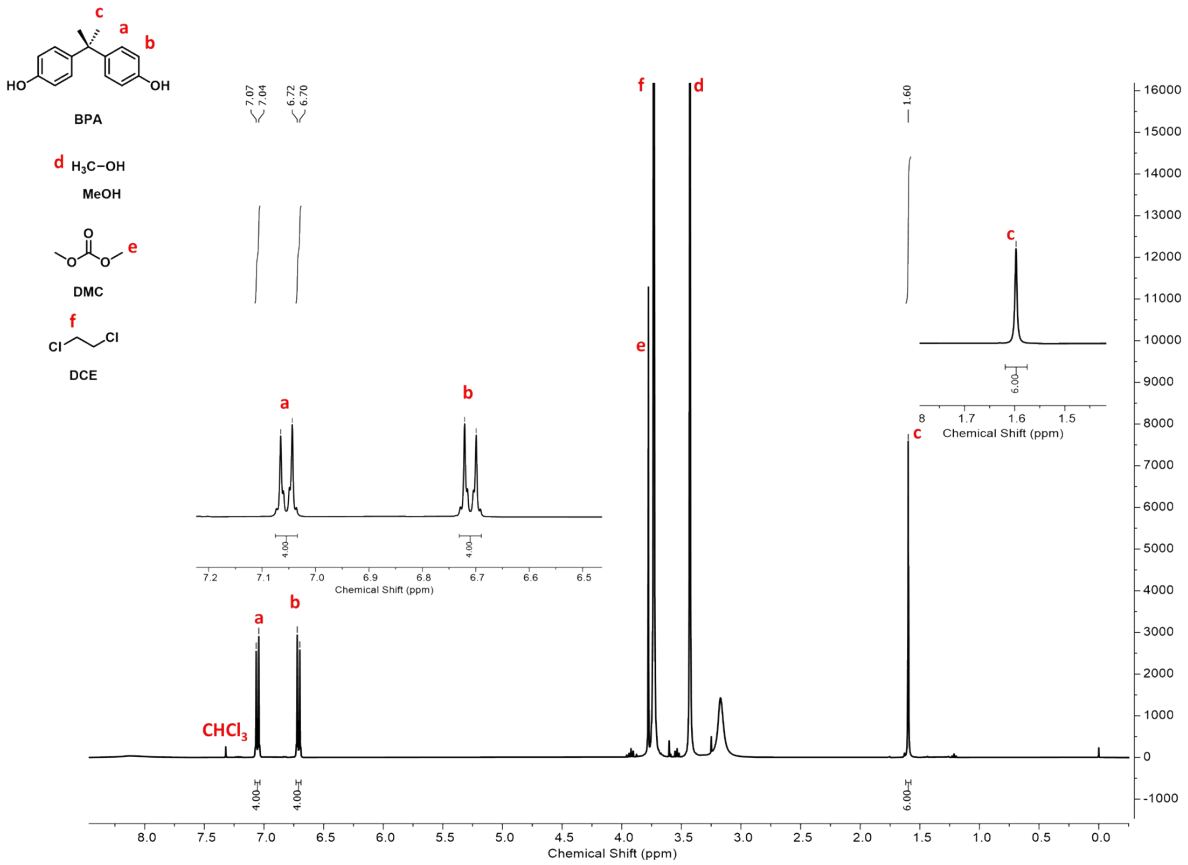

Figure S13. ^{1}H NMR spectrum (400 MHz, $CDCl_3$) of the BPA-PC methanolysis reaction mixture. Reaction condition: BPA-PC (0.5 g, 1.96 mmol), 8 equiv. methanol, 1 mL DCE, 12 wt.% CTO-500-5, 120 °C, 8 h. Resonances assigned as: **BPA-PC** Conv. = 100%; **BPA** (δ 7.08-7.03 (m, 4H), δ 6.73-6.69 (m, 4H), δ 1.60 (s, 6H)), Sel. = 100%.[1,2,3]

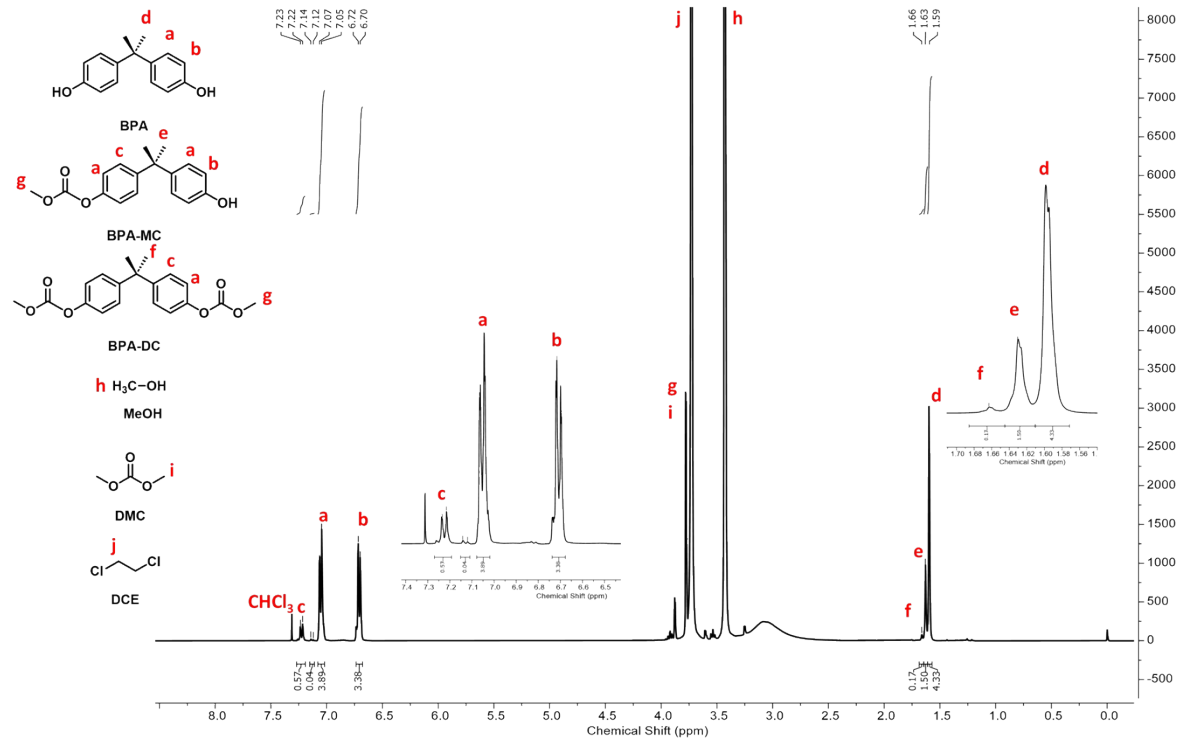

Figure S14. ^{1}H NMR spectrum (400 MHz, $CDCl_3$) of the BPA-PC methanolysis reaction mixture. Reaction condition: BPA-PC (0.5 g, 1.96 mmol), 8 equiv. methanol, 1 mL DCE, 12 wt.% CTO-500-3, 120 °C, 8 h. Resonances assigned as: **BPA-PC** Conv**.** = 100%; **BPA** (δ 7.08-7.03 (m, 4H), δ 6.73-6.69 (m, 4H), δ 1.60 (s, 6H)), Sel. = 72%; **BPA-MC** (δ 7.27-7.19 (m, 2H), δ 7.08-7.03 (m, 4H), δ 6.73-6.69 (m, 2H), δ 1.63 (s, 6H)), Sel. = 25%; **BPA-DC** (δ 7.27-7.19 (m, 4H), δ 7.08-7.03 (m, 4H), δ 1.66 (s, 6H)), Sel. = 3%.[1,2,3]

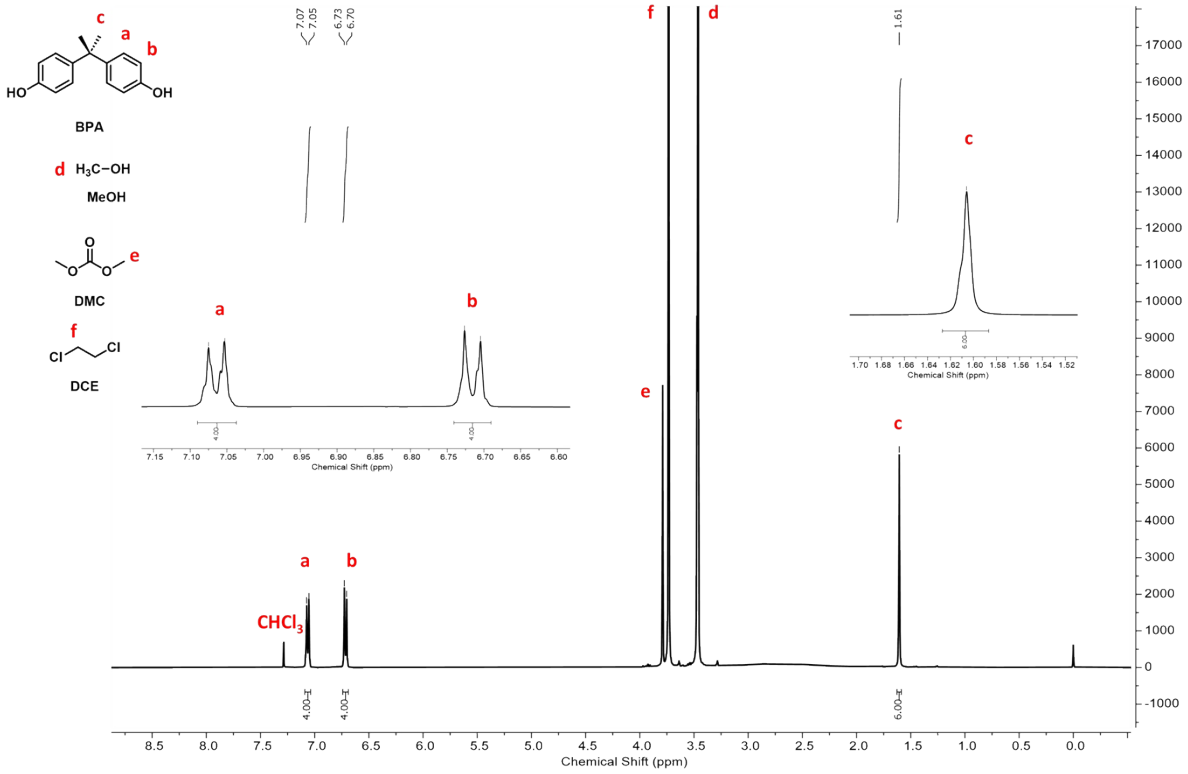

Figure S15. ^{1}H NMR spectrum (400 MHz, $CDCl_3$) of the BPA-PC methanolysis reaction mixture. Reaction condition: BPA-PC (0.5 g, 1.96 mmol), 8 equiv. methanol, 1 mL DCE, 12 wt.% CTO-500-7, 120 °C, 8 h. Resonances assigned as: **BPA-PC** Conv. = 100%; **BPA** (δ 7.08-7.03 (m, 4H), δ 6.74-6.69 (m, 4H), δ 1.61 (s, 6H)), Sel. = 100%.[1,2,3]

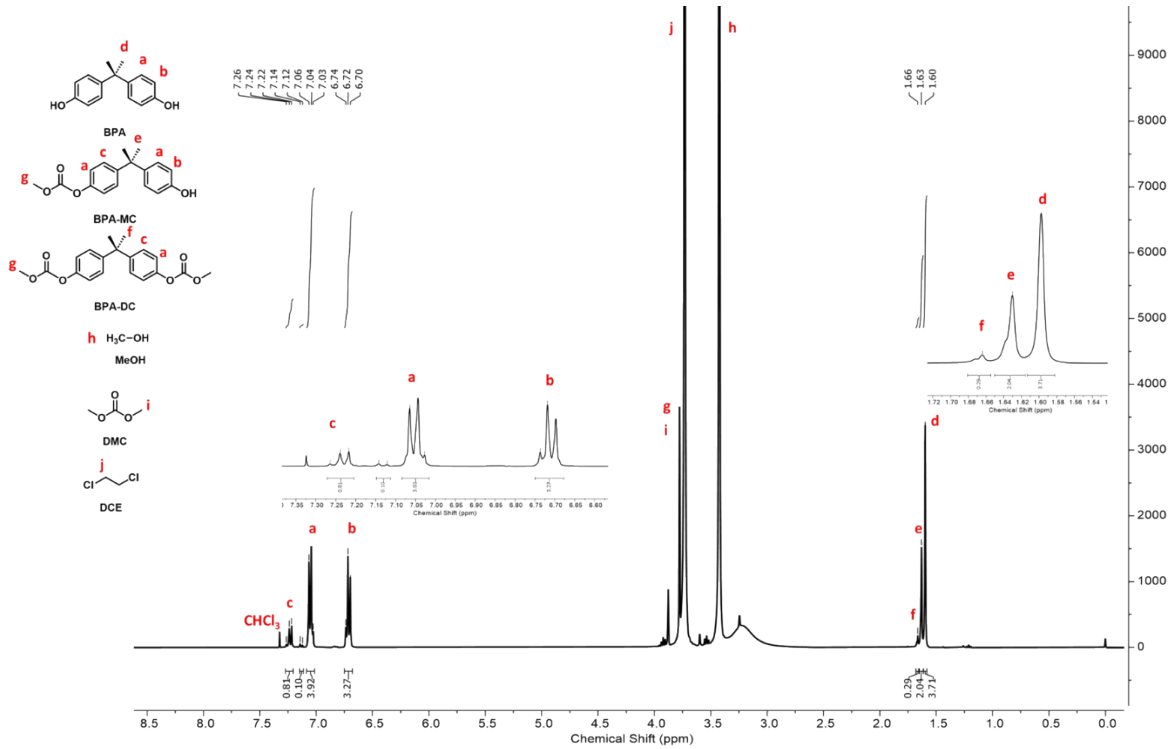

Figure S16. ^{1}H NMR spectrum (400 MHz, $CDCl_3$) of the BPA-PC methanolysis reaction mixture. Reaction condition: BPA-PC (0.5 g, 1.96 mmol), 8 equiv. methanol, 1 mL DCE, 12 wt.% CTO-500-10, 120 °C, 8 h. Resonances assigned as: **BPA-PC** Conv. = 100%; **BPA** (δ 7.09-7.01 (m, 4H), δ 6.75-6.69 (m, 4H), δ 1.60 (s, 6H)), Sel. = 62%; **BPA-MC** (δ 7.28-7.20 (m, 2H), δ 7.09-7.01 (m, 4H), δ 6.75-6.69 (m, 2H), δ 1.63 (s, 6H)), Sel. = 34%; **BPA-DC** (δ 7.28-7.20 (m, 4H), δ 7.09-7.01 (m, 4H), δ 1.66 (s, 6H)), Sel. = 4%.[1,2,3]

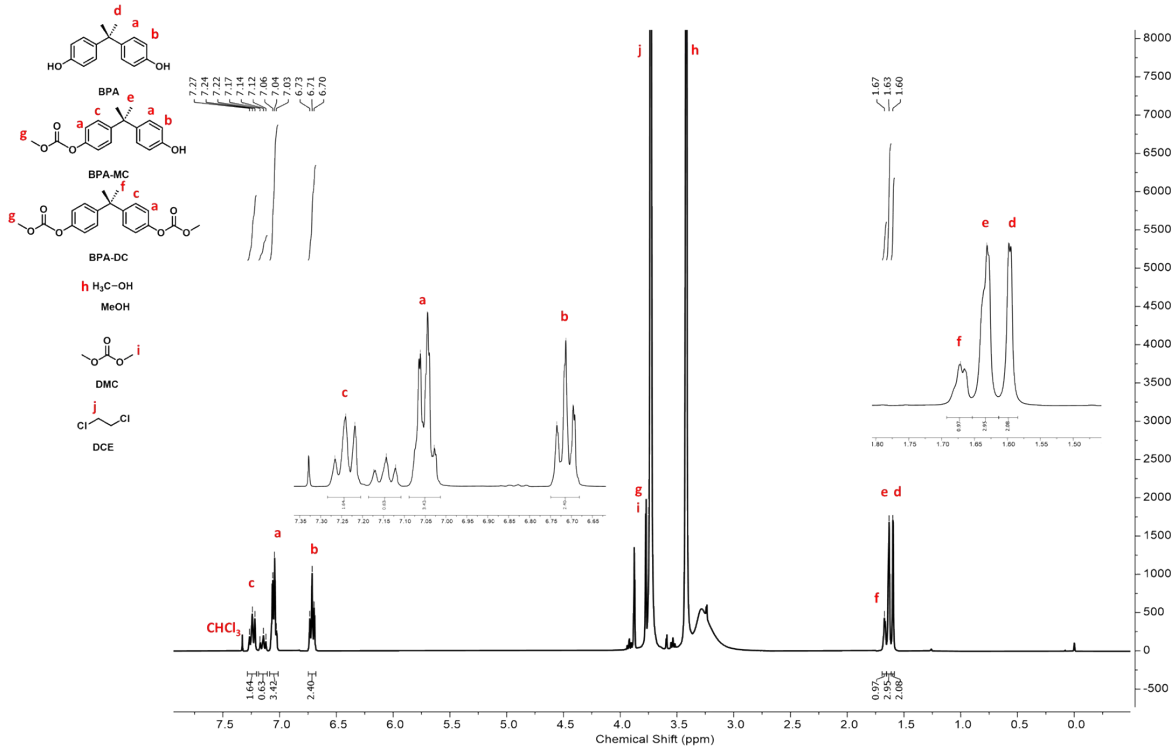

Figure S17. ^{1}H NMR spectrum (400 MHz, $CDCl_3$) of the BPA-PC methanolysis reaction mixture. Reaction condition: BPA-PC (0.5 g, 1.96 mmol), 8 equiv. methanol, 1 mL DCE, 12 wt.% CTO-550-3, 120 °C, 8 h. Resonances assigned as: **BPA-PC** Conv. = 100%; **BPA** (δ 7.09-

7.01 (m, 4H), δ 6.75-6.69 (m, 4H), δ 1.60 (s, 6H)), Sel. = 35%; **BPA-MC** (δ 7.28-7.20 (m, 2H), δ 7.09-7.01 (m, 4H), δ 6.75-6.69 (m, 2H), δ 1.63 (s, 6H)), Sel. = 49%; **BPA-DC** (δ 7.28-7.20 (m, 4H), δ 7.09-7.01 (m, 4H), δ 1.67 (s, 6H)), Sel. = 16%.[1,2,3]

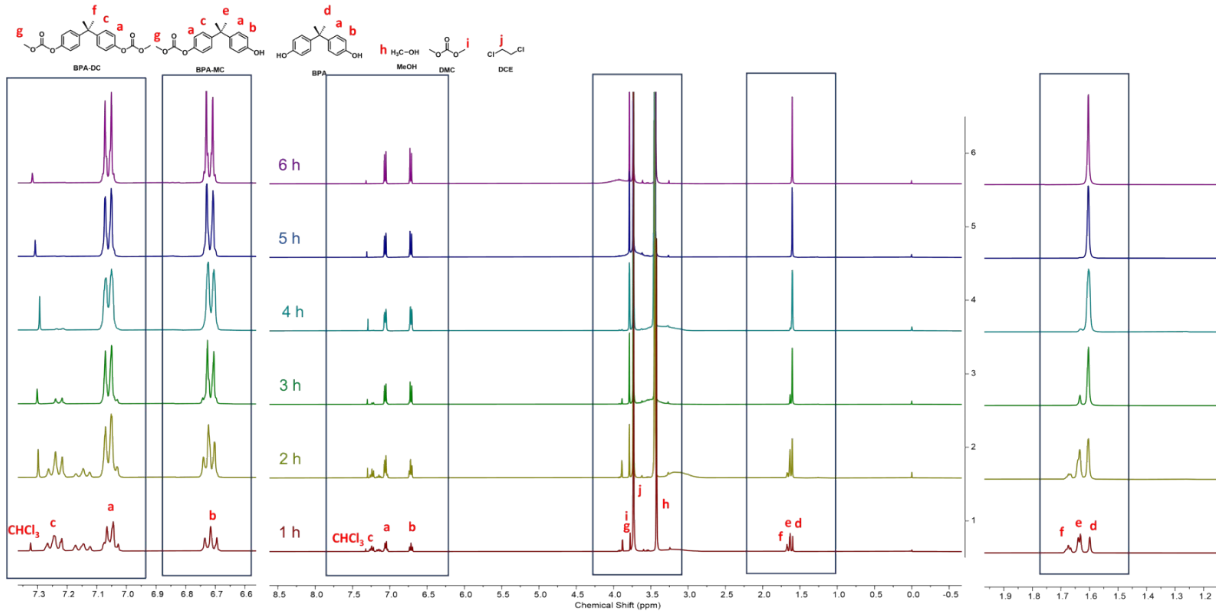

Figure S18. ^{1}H NMR spectra (400 MHz, $CDCl_3$) illustrating the reaction time screening for BPA-PC methanolysis. Reaction condition: BPA-PC (0.5 g, 1.96 mmol), 8 equiv. methanol, 1 mL DCE, 12 wt.% CTO-500-5, 120°C. **BPA-PC** Conv. = 68% (1 h);100% (2 h); 100% (3 h); 100% (4 h); 100% (5 h); 100% (6 h). **BPA** Sel. = 21% (1 h); 43% (2 h); 84% (3 h); 100% (4 h); 100% (5 h); 100% (6 h).

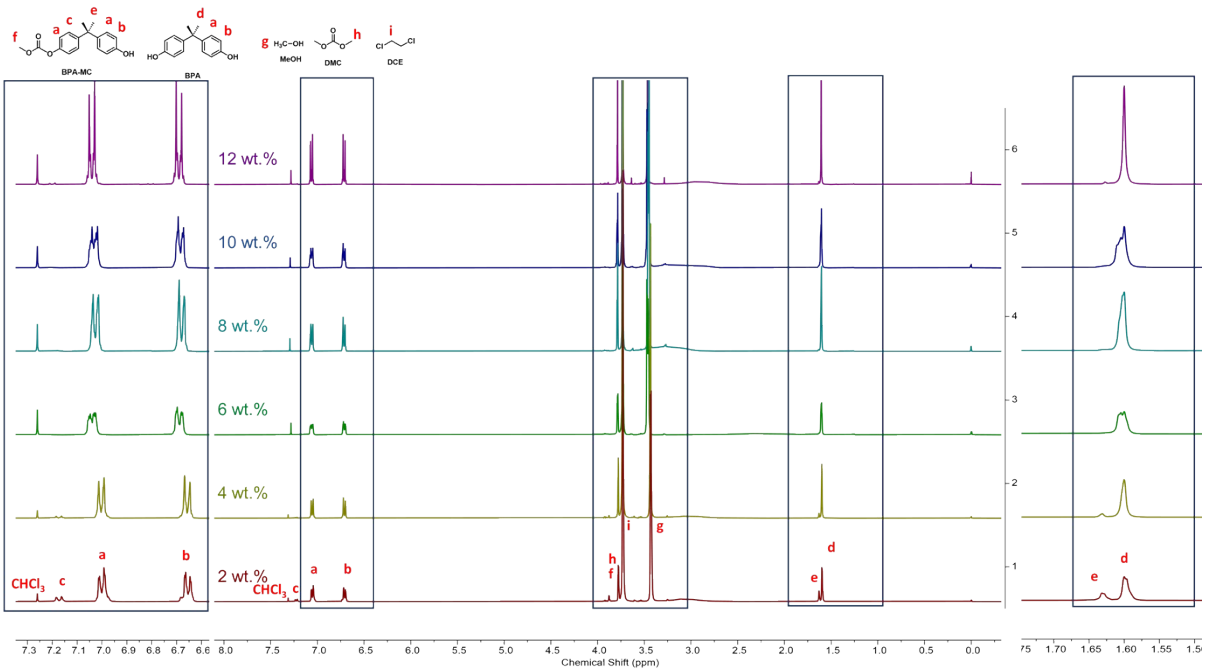

Figure S19. ^{1}H NMR spectra (400 MHz, $CDCl_3$) illustrating the catalyst loading screening for BPA-PC methanolysis. Reaction condition: BPA-PC (0.5 g, 1.96 mmol), 8 equiv. methanol, 1mL DCE, 120°C, 4h. **BPA-PC** Conv. = 100% (2 wt.%); 100% (4 wt.%); 100% (6 wt.%); 100% (8 wt.%); 100% (10 wt.%); 100% (12 wt.%). **BPA** Sel. = 76% (2 wt.%); 89% (4 wt.%); 100% (6 wt.%); 100% (8 wt.%); 100% (10 wt.%); 100% (12 wt.%).

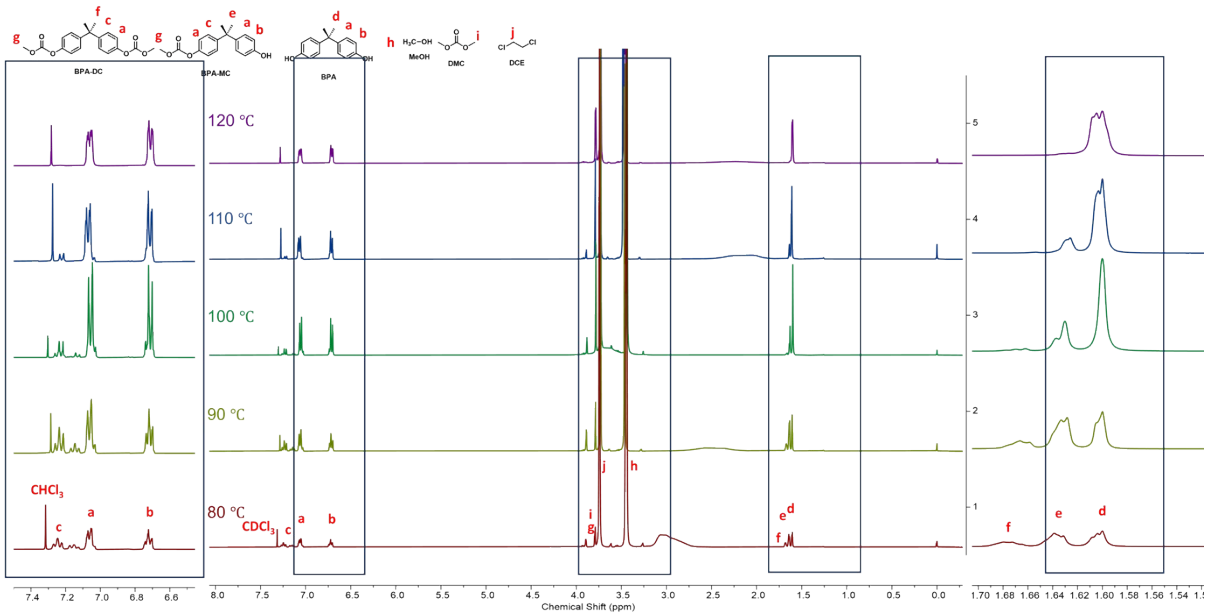

Figure S20. ^{1}H NMR spectra (400 MHz, $CDCl_3$) illustrating the reaction temperature screening for BPA-PC methanolysis. Reaction condition: BPA-PC (0.5 g, 1.96 mmol), 8 equiv. methanol 1 mL DCE, 6 wt.% CTO-500-5, 4 h. **BPA-PC** Conv. = 30% (80 °C); 76% (90 °C); 100% (100 °C); 100% (110 °C); 100% (120 °C). **BPA** Sel. = 36% (80 °C); 42% (90 °C); 69% (100 °C); 84% (110 °C); 100% (120 °C).

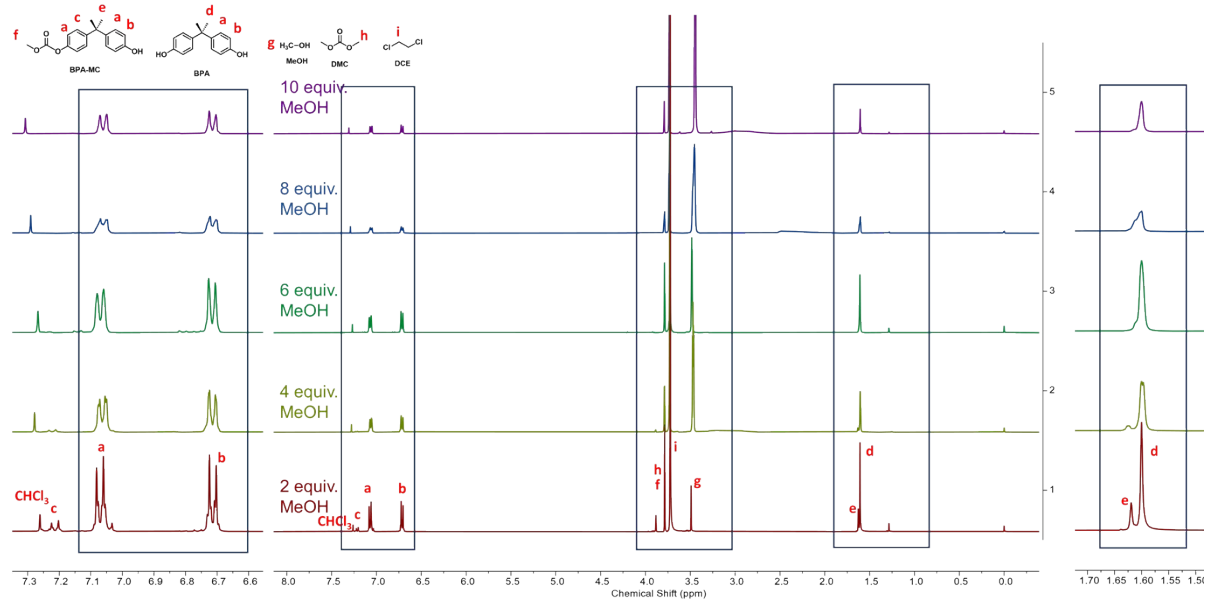

Figure S21. ^{1}H NMR spectra (400 MHz, $CDCl_3$) illustrating the methanol dosage screening for BPA-PC methanolysis. Reaction condition: BPA-PC (0.5 g, 1.96 mmol), 1 mL DCE, 6 wt.% CTO-500-5, 120°C, 4h. **BPA-PC** Conv. = 100% (2 equiv. MeOH); 100% (4 equiv. MeOH); 100% (6 equiv. MeOH); 100% (8 equiv. MeOH); 100% (10 equiv. MeOH). **BPA** Sel. = 78% (2 equiv. MeOH); 90% (4 equiv. MeOH); 100% (6 equiv. MeOH); 100% (8 equiv. MeOH); 100% (10 equiv. MeOH).

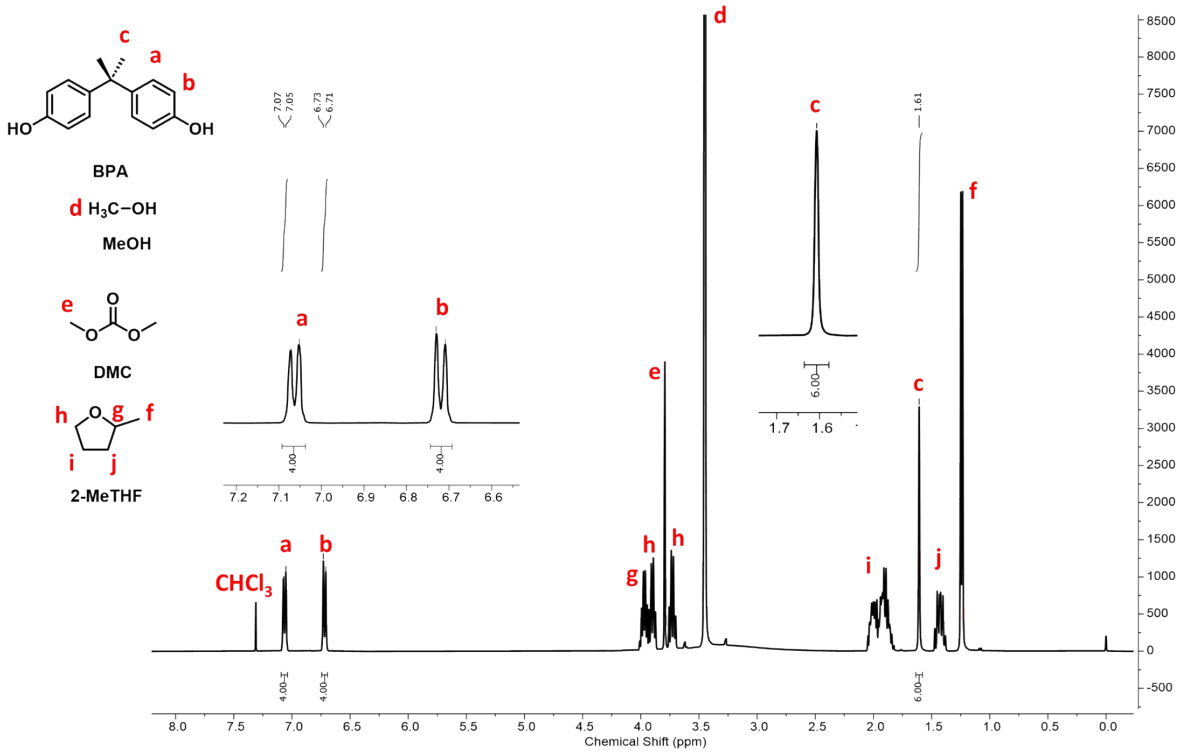

Figure S22. ^{1}H NMR spectrum (400 MHz, $CDCl_3$) of the BPA-PC methanolysis reaction mixture under **optimized conditions**. Reaction condition: BPA-PC (0.5 g, 1.96 mmol), 6 equiv. methanol, 1 mL 2-MeTHF, 6 wt.% CTO-500-5, 120 °C, 4 h. Resonances assigned as: **BPA-PC** Conv. = 100%; **BPA** (δ 7.08-7.03 (m, 4H), δ 6.73-6.69 (m, 4H), δ 1.60 (s, 6H)), Sel. = 100%.[1,2,3]

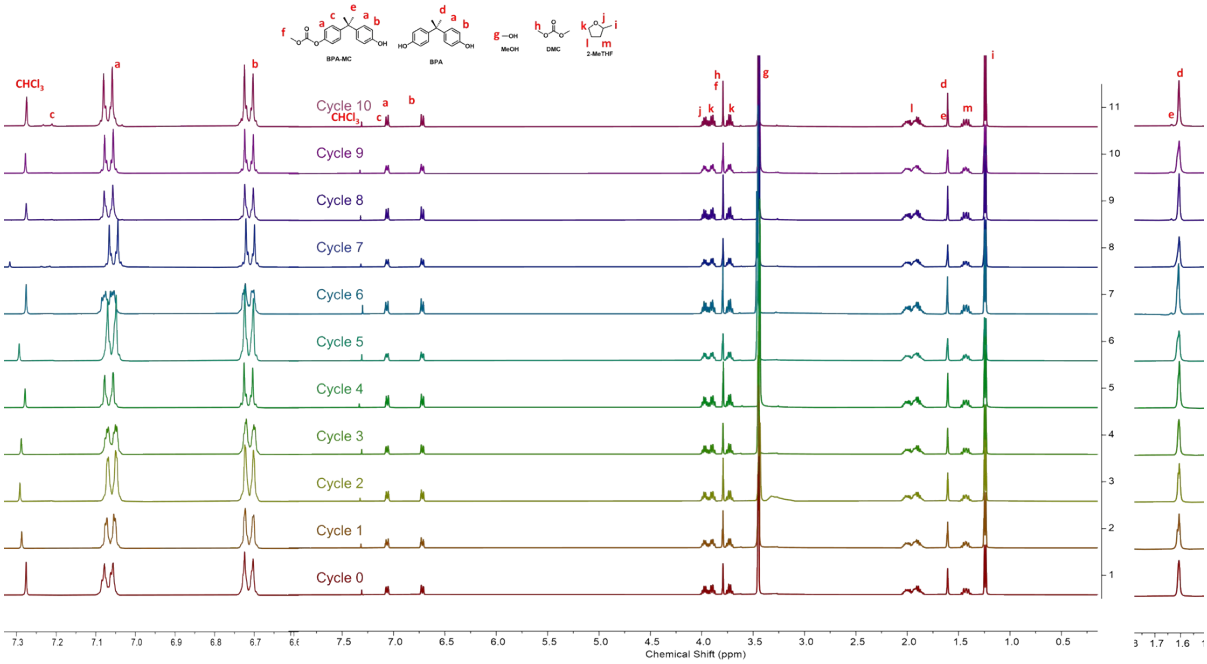

Figure S23. ^{1}H NMR spectra (400 MHz, $CDCl_3$) illustrating the recycling performance of CTO-500-5 for BPA-PC methanolysis. Reaction condition: BPA-PC (0.5 g, 1.96 mmol), 6 equiv. methanol, 1 mL 2-MeTHF, 6 wt.% CTO-500-5, 120°C, 4h. **BPA-PC** Conv. = 100% (cycle 0); 100% (cycle 1); 100% (cycle 2); 100% (cycle 3); 100% (cycle 4); 100% (cycle 5); 100% (cycle 6); 100% (cycle 7); 100% (cycle 8); 100% (cycle 9); 100% (cycle 10). **BPA** Sel.

= 100% (cycle 0); 100% (cycle 1); 100% (cycle 2); 100% (cycle 3); 100% (cycle 4); 100% (cycle 5); 98% (cycle 6); 97% (cycle 7); 97% (cycle 8); 96% (cycle 9); 95% (cycle 10).

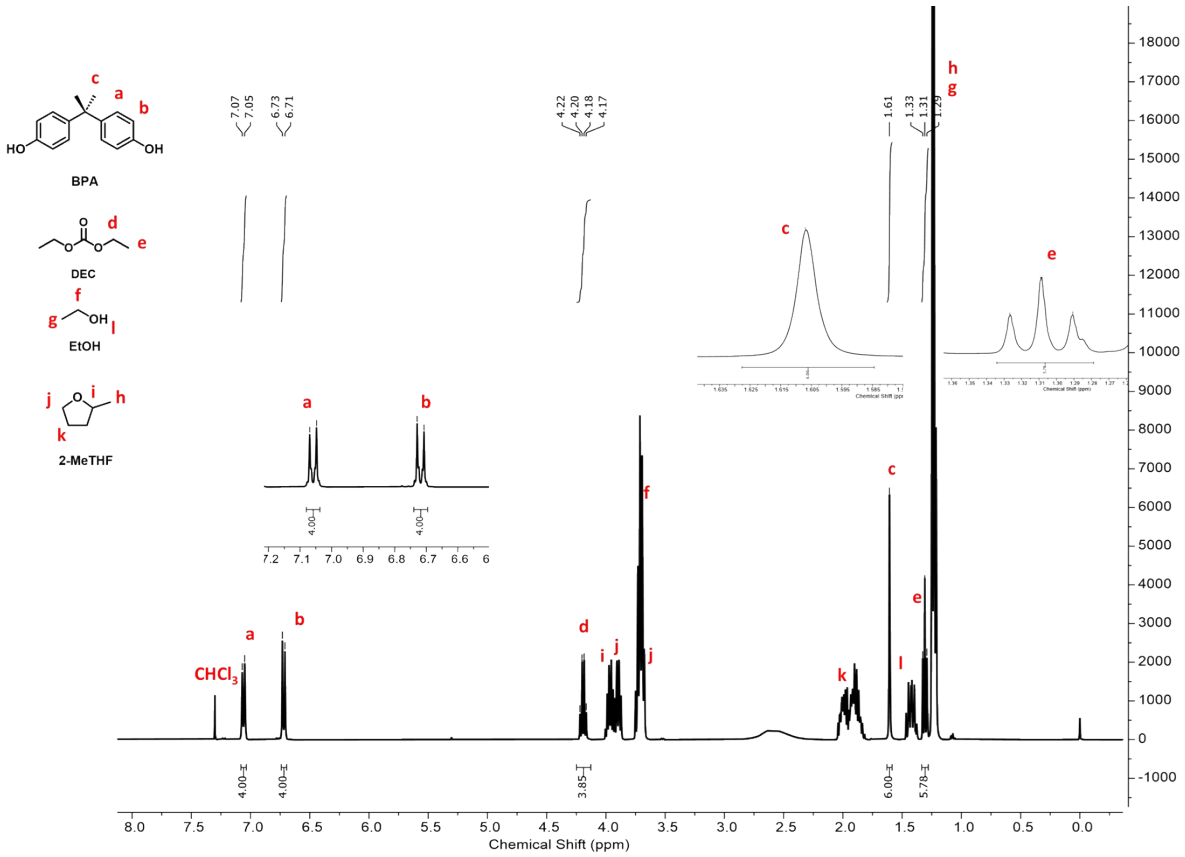

Figure S24. ^{1}H NMR spectrum (400 MHz, $CDCl_3$) of the BPA-PC ethanolysis reaction mixture. Reaction condition: BPA-PC (0.5 g, 1.96 mmol), 10 equiv. EtOH, 1 mL 2-MeTHF, 6 wt.% CTO-500-5, 160 °C, 4 h. Resonances assigned as: **BPA-PC** Conv. = 100%; **BPA** (δ 7.08-7.03 (m, 4H), δ 6.74-6.69 (m, 4H), δ 1.60 (s, 6H)), Sel. = 100%; **Diethyl carbonate (DEC)** (δ 4.23-4.14 (s, 4H), δ 1.33-1.28 (m, 6H)), Sel. = 96%.[3]

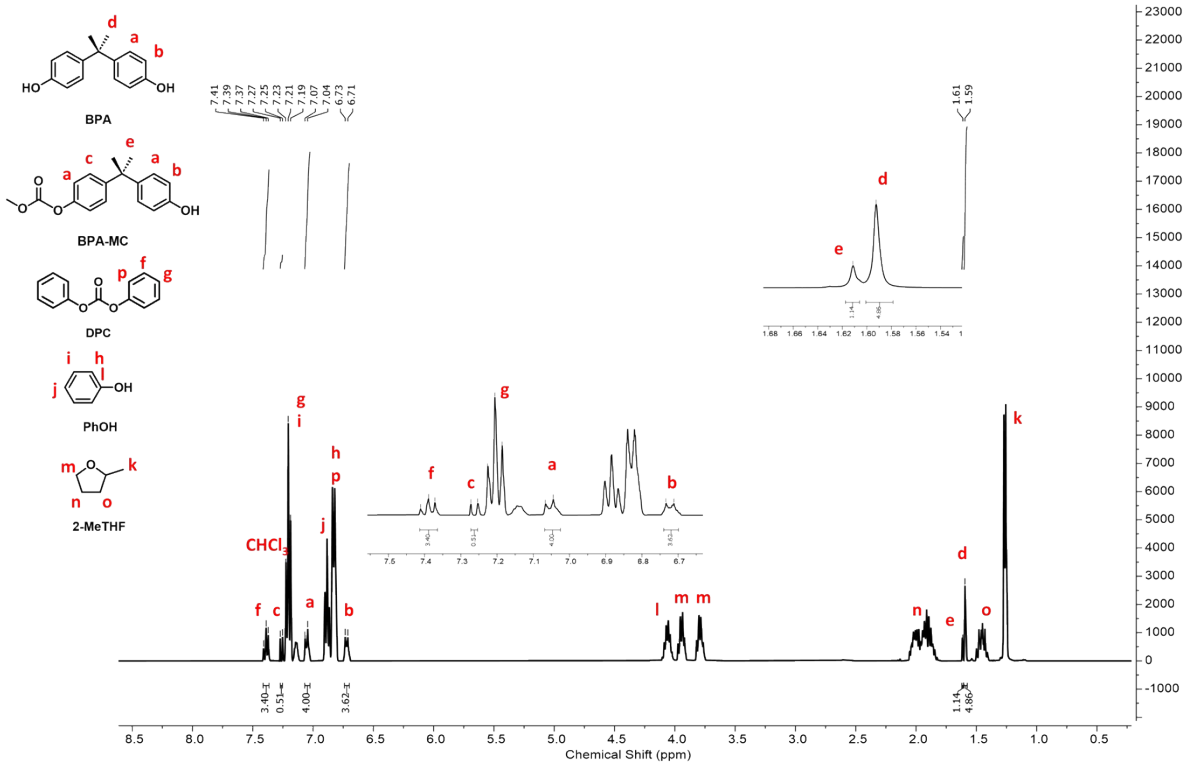

Figure S25. ^{1}H NMR spectrum (400 MHz, $CDCl_3$) of the BPA-PC phenolysis reaction mixture. Reaction condition: BPA-PC (0.5 g, 1.96 mmol), 10 equiv. PhOH, 1 mL 2-MeTHF, 6 wt.% CTO-500-5, 160 °C, 4 h. Resonances assigned as: **BPA-PC** Conv. = 100%; **BPA** (δ 7.08-7.03 (m, 4H), δ 6.72-6.68 (m, 4H), δ 1.60 (s, 6H)), Sel. = 81%; **BPA-MC** (δ 7.28-7.20 (m, 2H), δ 7.09-7.01 (m, 4H), δ 6.75-6.69 (m, 2H), δ 1.63 (s, 6H)), Sel. = 19%; **Diphenyl carbonate (DPC)** (δ 7.41-7.35 (m, 4H), δ 7.26-7.24 (m, 6H)), Sel. = 85%.[4]

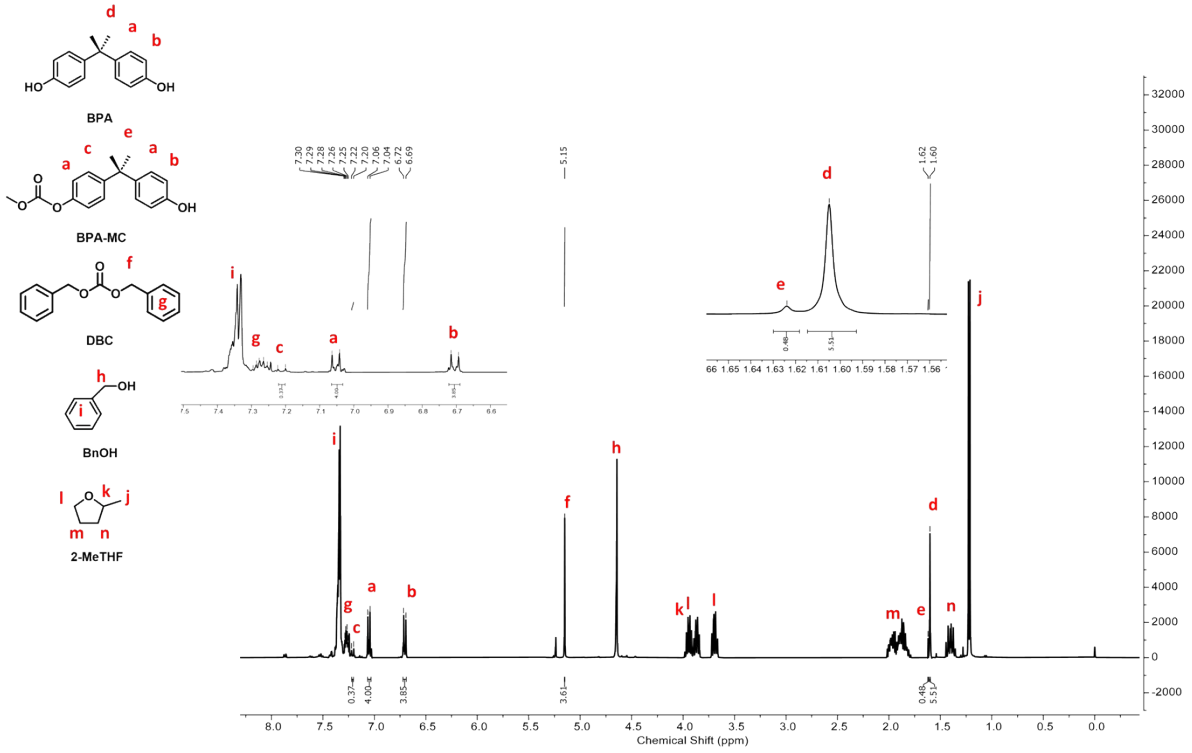

Figure S26. ^{1}H NMR spectrum (400 MHz, $CDCl_3$) of the BPA-PC benzyl alcoholysis reaction

mixture. Reaction condition: BPA-PC (0.5 g, 1.96 mmol), 10 equiv. BnOH, 1 mL 2-MeTHF, 6 wt.% CTO-500-5, 160 °C, 4 h. Resonances assigned as: **BPA-PC** Conv. = 100%; **BPA** (δ 7.08-7.03 (m, 4H), δ 6.72-6.68 (m, 4H), δ 1.60 (s, 6H)), Sel. = 92%; **BPA-MC** (δ 7.28-7.20 (m, 2H), δ 7.09-7.01 (m, 4H), δ 6.75-6.69 (m, 2H), δ 1.63 (s, 6H)), Sel. = 8%; **Dibenzyl carbonate (DBC)** (δ 7.32-7.26 (m, 10H), δ 5.16 (s, 4H)), Sel. = 90%.[4]

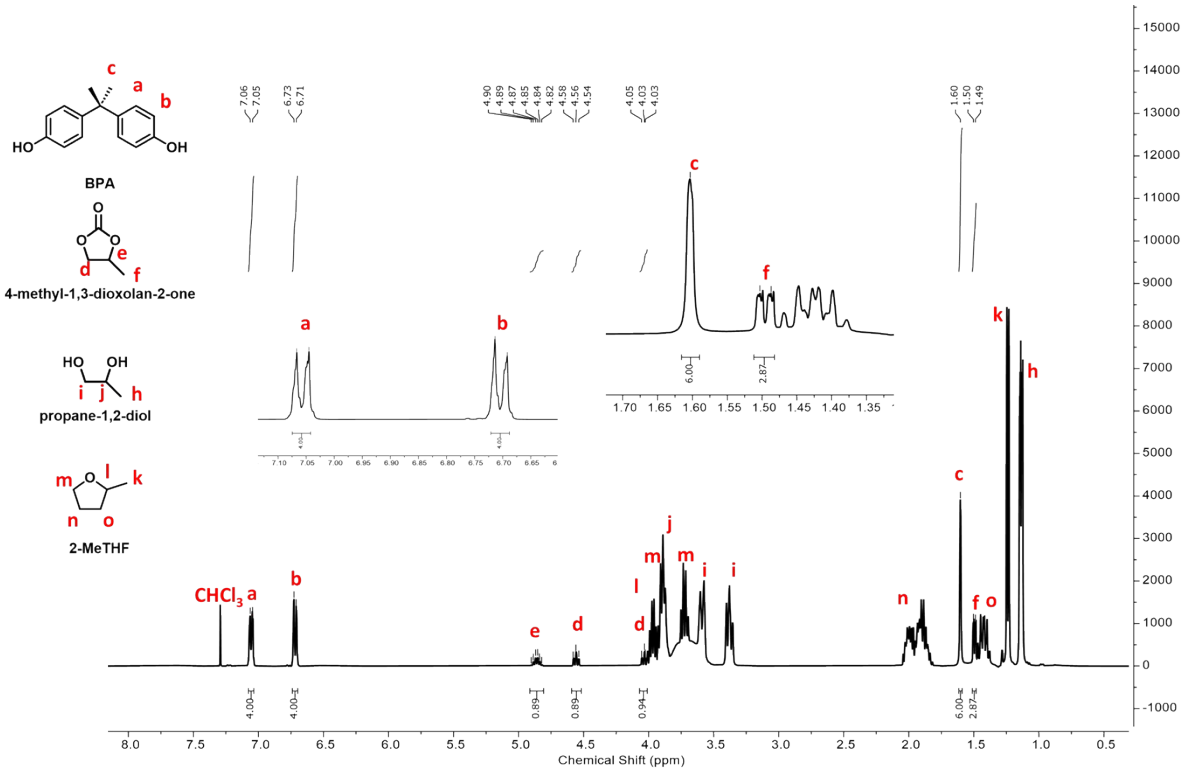

Figure S27. ^{1}H NMR spectrum (400 MHz, $CDCl_3$) of the BPA-PC 1,2-propanediolysis reaction mixture. Reaction condition: BPA-PC (0.5 g, 1.96 mmol), 3 equiv. 1,2-propanediol, 1 mL 2-MeTHF, 6 wt.% CTO-500-5, 120 °C, 4 h. Resonances assigned as: **BPA-PC** Conv. = 100%; **BPA** (δ 7.08-7.03 (m, 4H), δ 6.72-6.68 (m, 4H), δ 1.60 (s, 6H)), Sel. = 100%; **4-methyl-1,3-dioxolan-2-one** (δ 4.91-4.80 (m, 1H), δ 4.58-4.52 (m, 1H), δ 4.06-4.00 (m, 1H), δ 1.51-1.48 (m, 3H)), Sel. = 96%.[3,5,6]

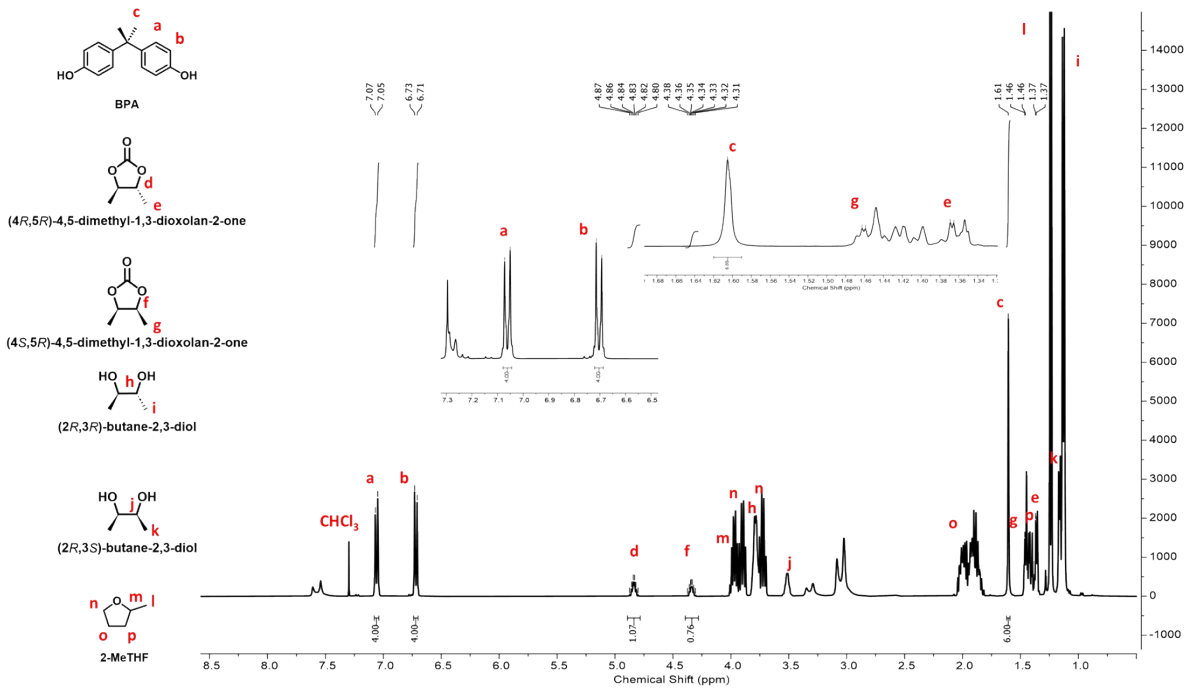

Figure S28. ^{1}H NMR spectrum (400 MHz, $CDCl_3$) of the BPA-PC 2,3-butanediolysis reaction mixture. Reaction condition: BPA-PC (0.5 g, 1.96 mmol), 3 equiv. 2,3-butanediol, 1 mL 2-MeTHF, 6 wt.% CTO-500-5, 120 °C, 4 h. Resonances assigned as: **BPA-PC** Conv. = 100%; **BPA** (δ 7.08-7.03 (m, 4H), δ 6.72-6.68 (m, 4H), δ 1.61 (s, 6H)), Sel. = 100%; **4,5-dimethyl-1,3-dioxolan-2-one** The reaction yielded two stereoisomeric cyclic carbonates, (R,S)-isomers (δ 4.88-4.79 (m, 2H), δ 1.38-1.35 (m, 6H)); (S,R)-isomers (δ 4.38-4.29 (m, 2H), δ 1.47-1.44 (m, 6H)), Sel. = 92%.[5]

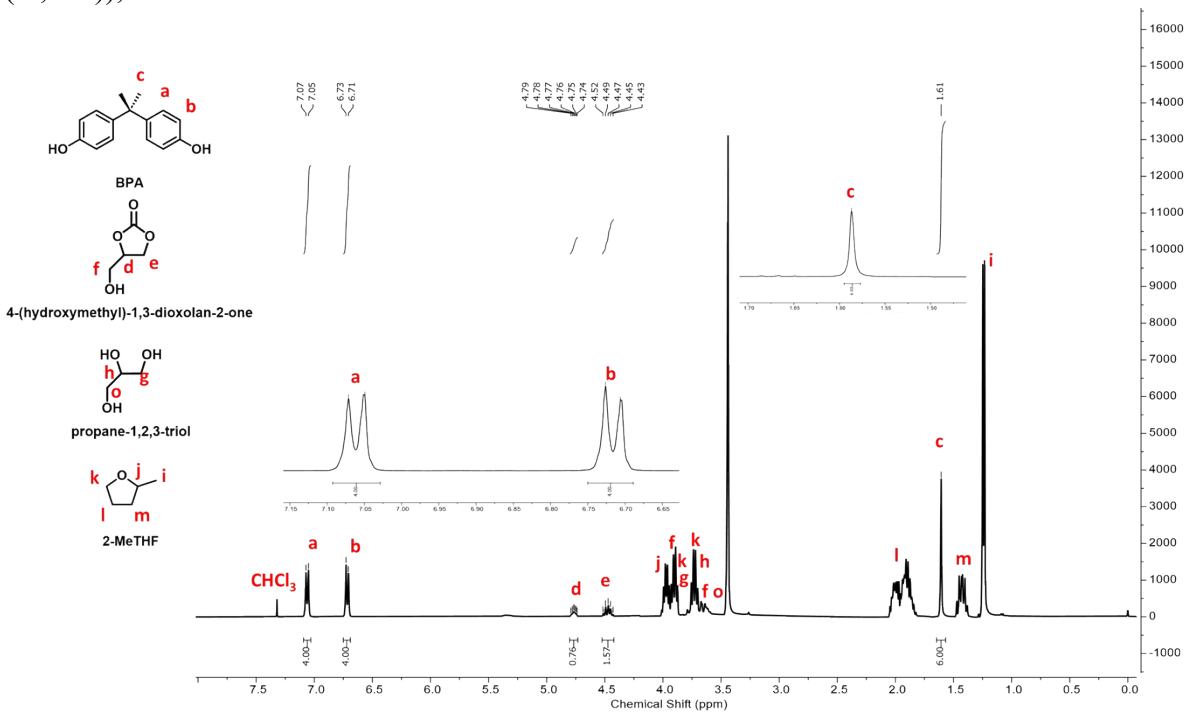

Figure S29. ^{1}H NMR spectrum (400 MHz, $CDCl_3$) of the BPA-PC glycerolysis reaction mixture. Reaction condition: BPA-PC (0.5 g, 1.96 mmol), 4 equiv. glycerol, 1 mL 2-MeTHF, 6 wt.% CTO-500-5, 120 °C, 4 h. Resonances assigned as: **BPA-PC** Conv. = 100%; **BPA** (δ 7.08-7.03 (m, 4H), δ 6.72-6.68 (m, 4H), δ 1.59 (s, 6H)), Sel. = 100%; **4-(hydroxymethyl)-1,3-**

dioxolan-2-one (δ 4.80-4.69 (m, 1H), δ 4.52-4.39 (m, 2H), δ 4.00-3.85 (m, 1H), δ 3.74-3.72 (m, 1H)), Sel. = 78%.[5,6]

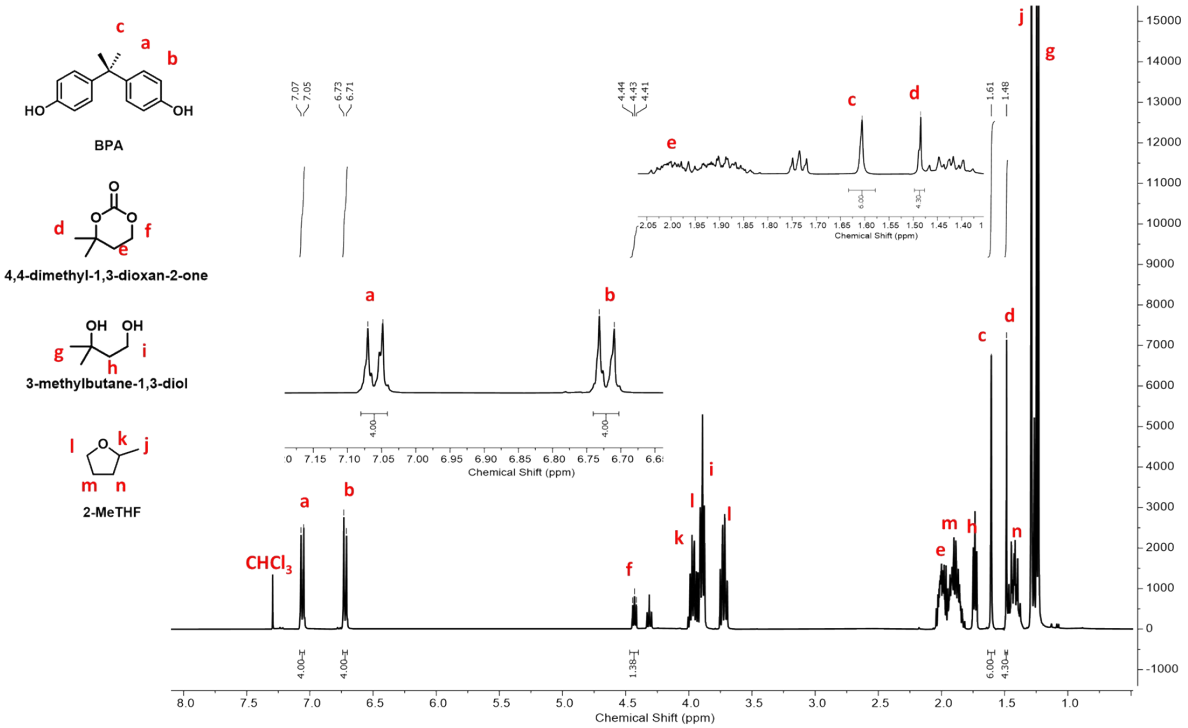

Figure S30. ^{1}H NMR spectrum (400 MHz, $CDCl_3$) of the BPA-PC 3-methyl-1,3-butanediolysis reaction mixture. Reaction condition: BPA-PC (0.5 g, 1.96 mmol), 1.5 equiv. 3-methyl-1,3-butanediol, 1 mL 2-MeTHF, 6 wt.% CTO-500-5, 130 °C, 4 h. Resonances assigned as: **BPA-PC** Conv. = 100%; **BPA** (δ 7.08-7.03 (m, 4H), δ 6.73-6.68 (m, 4H), δ 1.61 (s, 6H)), Sel. = 84%; **BPA-MC** (δ 7.28-7.20 (m, 2H), δ 7.09-7.01 (m, 4H), δ 6.75-6.69 (m, 2H), δ 1.64 (s, 6H)), Sel. = 16%; **4,4-dimethyl-1,3-dioxan-2-one** (δ 4.45-4.40 (m, 2H), δ 2.03-1.98 (m, 2H), δ 1.49 (s, 6H)), Sel. = 72%.[6]

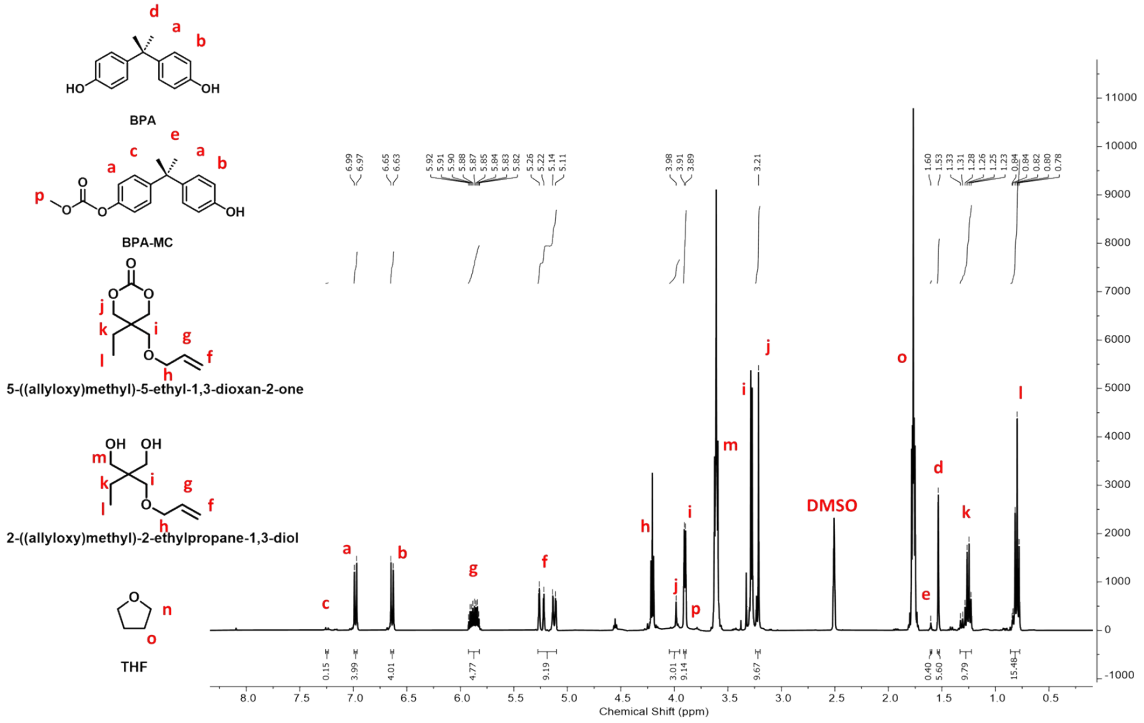

Figure S31. ^{1}H NMR spectrum (400 MHz, DMSO-*d6*) of the BPA-PC 2-((allyloxy)methyl)-2-ethylpropane-1,3-diolysis reaction mixture. Reaction condition: BPA-PC (0.5 g, 1.96 mmol), 2 equiv. 2-((allyloxy)methyl)-2-ethylpropane-1,3-diol, 1 mL THF, 6 wt.% CTO-500-5, 120 °C, 4 h. Resonances assigned as: **BPA-PC** Conv. = 100%; **BPA** (δ 7.08-7.03 (m, 4H), δ 6.73-6.68 (m, 4H), δ 1.61 (s, 6H)), Sel. = 93%; **BPA-MC** (δ 7.28-7.20 (m, 2H), δ 7.09-7.01 (m, 4H), δ 6.75-6.69 (m, 2H), δ 1.64 (s, 6H)), Sel. = 7%; **5-((allyloxy)methyl)-5-ethyl-1,3-dioxan-2-one (AOMEC)** (δ 5.92-5.83 (m, 1H), δ 5.27-5.10 (m, 2H), δ 3.98 (s, 4H), δ 3.91 (s, 2H), δ 3.21 (s, 2H), δ 1.39 (m, 2H), δ 0.84 (m, 6H)), Sel. = 75%.[6,7]

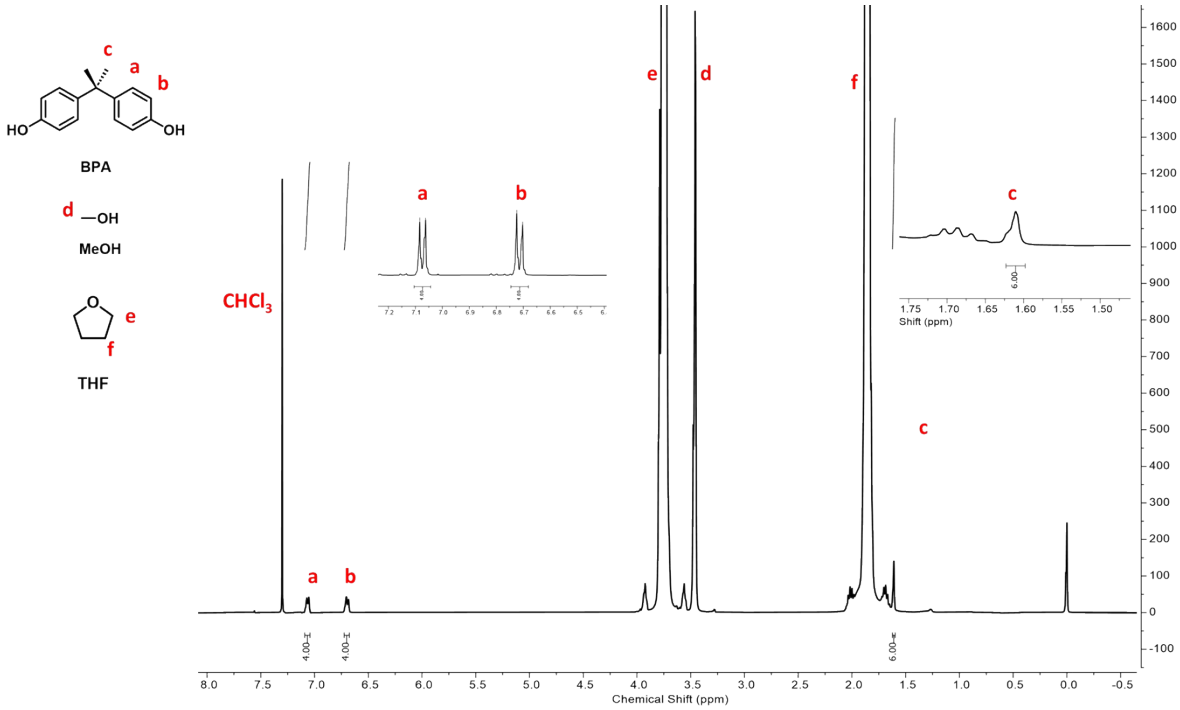

Figure S32. ^{1}H NMR spectrum (400 MHz, $CDCl_3$) of the BPA-PC methanolysis effluent collected from the continuous fixed-bed flow reactor under **optimized conditions**. Resonances assigned as: **BPA-PC** Conv. = 100%; **BPA** (δ 7.09-7.06 (m, 4H), δ 6.74-6.69 (m, 4H), δ 1.61 (s, 6H)), Sel. = 100%.[1,2,3]

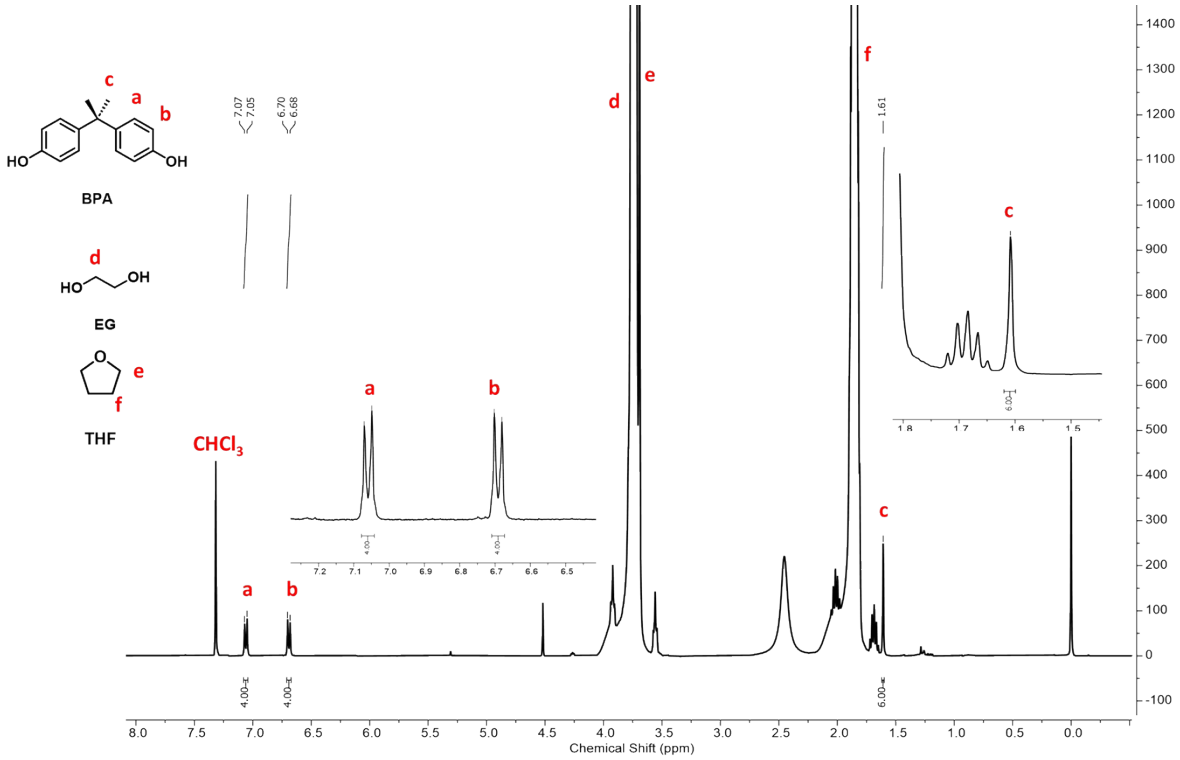

Figure S33. ^{1}H NMR spectrum (400 MHz, $CDCl_3$) of the BPA-PC glycolysis effluent collected from the continuous fixed-bed flow reactor under **optimized conditions**. Resonances assigned as: **BPA-PC** Conv. = 100%; **BPA** (δ 7.09-7.05 (m, 4H), δ 6.72-6.67 (m, 4H), δ 1.61 (s, 6H)), Sel. = 100%.[1,2,3]

6. References

[1] Z. Wang, R. Yang, G. Xu, T. Liu, Q. Wang, Chemical upcycling of poly(bisphenol A carbonate) plastic catalyzed by ZnX_2 via an amino-alcoholysis strategy, ACS Sustain. Chem. Eng. 10 (2022) 4529–4537, https://doi.org/10.1021/acssuschemeng.1c08408

[2] M. Edge, N. Yadav, A.A.R. Hmayed, A.P. Dove, A. Brandolese, Continuous flow depolymerization of polycarbonates and poly(lactic acid) promoted by supported organocatalysts, ChemSusChem 18 (2025) e202500420, https://doi.org/10.1002/cssc.202500420

[3] T. Do, E.R. Baral, J.G. Kim, Chemical recycling of poly(bisphenol A carbonate): 1,5,7-triazabicyclo[4.4.0]-dec-5-ene catalyzed alcoholysis for highly efficient bisphenol A and organic carbonate recovery, Polymer 143 (2018) 106–114, https://doi.org/10.1016/j.polymer.2018.04.015

[4] F. Iannone, M. Casiello, A. Monopoli, P. Cotugno, M.C. Sportelli, R.A. Picca, N. Cioffi, M.M. Dell'Anna, A. Nacci, Ionic liquids/ZnO nanoparticles as recyclable catalyst for polycarbonate depolymerization, J. Mol. Catal. A Chem. 426 (2017) 107–116, https://doi.org/10.1016/j.molcata.2016.11.006

[5] I.E. Nifant'ev, D.A. Pyatakov, A.N. Tavtorkin, P.V. Ivchenko, Chemical recycling and upcycling of poly(bisphenol A carbonate) via metal acetate catalyzed glycolysis, Polym. Degrad. Stab. 207 (2023) 110210, https://doi.org/10.1016/j.polymdegradstab.2022.110210

[6] C. Jehanno, J. Demarteau, D. Mantione, M.C. Arno, F. Ruipérez, J.L. Hedrick, A.P. Dove, H. Sardon, Synthesis of functionalized cyclic carbonates through commodity polymer upcycling, ACS Macro Lett. 9 (2020) 443–447, https://doi.org/10.1021/acsmacrolett.0c00164

[7] C. Jehanno, J. Demarteau, D. Mantione, M.C. Arno, F. Ruipérez, J.L. Hedrick, A.P. Dove, H. Sardon, Selective chemical upcycling of mixed plastics guided by a thermally stable organocatalyst, Angew. Chem. Int. Ed. 60 (2021) 1460–1468, https://doi.org/10.1002/anie.202014860